Mitochondrial Transplantation: Adaptive Bio-enhancement

Xiaomeng Lu[1], Yong Jiang[2]
[1]Guangdong Provincial Key Laboratory of Proteomics, School of Basic Medical Sciences, Southern Medical University; Guangzhou, 510515, China.
[2]Guangdong Provincial Key Laboratory of Proteomics, School of Basic Medical Sciences, Southern Medical University; Guangzhou, 510515, China.

Abstract

Mitochondria, known as the powerhouse of the cell, are essential for cellular energy production. Dysfunction in mitochondrial function can significantly affect various organs. Transplanting healthy mitochondria can enhance the bioenergetics of diseased cells and treat various conditions, yet the limits of mitochondrial transplantation are still unknown. Our study reveals that the source of transplanted mitochondria is not restricted by species, and recipient cells show no significant immune response to mitochondria from different lineages. We also found that metabolic compatibility between the recipient and exogenous mitochondria is crucial, and transplanting mitochondria from different species can endow recipient cells with distinct characteristics to combat diseases. Furthermore, our data indicate that there is competition among mitochondria with varying functions, with more powerful mitochondria yielding better therapeutic effects. Notably, we have not yet found an upper limit for the bio-enhancement provided by exogenous mitochondria. Our research proposes a feasible path for human bio-enhancement through mitochondrial transplantation—adaptive bio-enhancement.

Key words: mitochondrial transplantation, immune response, metabolic compatibility, competition, mitochondrial function, bio-enhancement
Subject Categories: Biotechnology, Cell Metabolism, Organelle Transplantation

Mitochondrial transplantation is a highly clinically valuable technique. I have further expanded the variety of mitochondrial sources for transplantation and demonstrated the potential of mitochondrial transplantation to adaptively enhance biological functions.

Introduction

Mitochondrial transplantation involves isolating mitochondria from normal cells or tissues and transferring them to diseased areas either directly or indirectly to improve the function of damaged cells, thereby aiding in treatment. Compared to organ, tissue, or cell transplantation, mitochondrial transplantation is a novel and milder alternative therapy. In 2009, Boston Children 's Hospital first reported mitochondrial transplantation, injecting mitochondria into ischemic regions of the rabbit heart and observing significant therapeutic effects(McCully, Cowan et al., 2009). To date, mitochondrial transplantation has shown promising therapeutic outcomes in various organ and tissue injuries, including the heart(Gorick & Debski, 2024, Moskowitzova, Shin et al., 2019), brain(Eo, Yu et al., 2024, Sun, Zhao et al., 2024), spinal cord(Zhu, Li et al., 2023), lungs, kidneys(Su, Zhu et al., 2016), liver(Ulger, Kubat et al., 2021), skeletal muscle(Lee, Hwang et al., 2021), and skin(Li, Cao et al., 2024), as well as in conditions such as sepsis(Kim, Noh et al., 2023) and cancer(Cruz-Gregorio, Aranda-Rivera et al., 2023).

Despite the proven safety and therapeutic efficacy of mitochondrial transplantation in numerous diseases(Hosseinian, Ali Pour et al., 2022), its full potential remains unclear. Transplanting functionally normal mitochondria to restore the function of dysfunctional mitochondria in diseased cells involves differences in mitochondrial function, which enhances the function of diseased cells. Preemptively providing normal cells with exogenous mitochondria can grant them a higher damage threshold, thereby bioenergetically enhancing normal cells(Boutonnet, Mallard et al., 2024, Moskowitzova et al., 2019). The question arises: can we select mitochondria with different characteristics for different disease populations or use mitochondria with functions superior to normal mitochondria as a purely adaptive bio-enhancement strategy? This is a topic worth exploring.

In this study, we expanded the sources of mitochondria for transplantation and demonstrated the universality of mitochondrial transplantation. We further utilized the lineage-specific characteristics of mitochondria to treat cells under different disease conditions, highlighting the importance of metabolic matching. Additionally, we obtained hybrid mitochondria with enhanced therapeutic suitability by inducing cell fusion to combine multiple lineage characteristics. Building on this, we discovered that mitochondria with greater functional potency exhibited an overwhelmingly superior therapeutic effect compared to their lineage-specific counterparts, even enhancing the function of normal cells to some extent. Similar results were observed in animal experiments, suggesting that mitochondrial transplantation could potentially be used as a means of biological enhancement. This significantly broadens the therapeutic value of mitochondrial transplantation and offers a new research direction for biological augmentation.

Results

Universality of Mitochondrial Transplantation

Mitochondria, a fundamental and essential organelle present in most eukaryotic cells, have a relatively simple genome structure, typically ranging in size from 15 to 60 kb. Their primary function is to supply energy to cells(Gray, Burger et al., 1999, Schatz, 2012). The prevailing theory suggests that mitochondria originated from α-proteobacteria that established a stable endosymbiotic relationship with the host during the process of organelle formation. As the α-proteobacteria progressively reduced their protein repertoire and transferred most of their genetic material to the host nucleus(Gray et al., 1999), this unique evolutionary process likely explains why mitochondria, even when transplanted between different species or across species, do not elicit significant immune or inflammatory responses(Ali Pour, Kenney et al., 2020, Doulamis, Guariento et al., 2020, Jiang, Elliott et al., 2015). Current research on mitochondrial transplantation primarily uses mitochondria from three sources: various cell lines(Chang, Chang et al., 2019, Chen, Majerníková et al., 2023, Sun, Liu et al., 2019, Sun, Gao et al., 2021), human umbilical cord mesenchymal stem cells(Yao, Ma et al., 2022), and tissues such as liver(Yu, Hou et al., 2021), skeletal muscle(Bhattacharya, Slavin et al., 2023),, brain(Picone, Porcelli et al., 2021), and platelets(Baharvand, Habibi Roudkenar et al., 2024), with the experimental animals mainly being humans(Bamshad, Habibi Roudkenar et al., 2023, Guariento, Piekarski et al., 2021), rabbits(McCully et al., 2009), mice(Dubinin, Mikheeva et al., 2024), pigs(Kaza, Wamala et al., 2017), and rats(Javani, Babri et al., 2022). We aimed to expand the species origin of mitochondria used for transplantation to enhance the therapeutic potential of this approach.

Using green fluorescent markers, we labeled mitochondria from 13 different animal species, including African green monkey kidney cells(Vero), bovine kidney cells(MDCK), MDBK canine kidney cells(MDBK), feline kidney cells(CRFK), porcine kidney cells(PK15), chicken hepatocarcinoma cells(LMH), Spodoptera frugiperda cells (Sf9), turtle liver tissue, bullfrog liver tissue, quail liver tissue, lizard liver tissue, large yellow croaker liver tissue, and eel liver tissue. Through ATP assays (Figure 1A), JC-1 staining (Figure 1B), transmission electron microscopy (Figure 1C), and mitochondrial respiratory chain complex activity assays (Figures 1D-G), we confirmed that the isolated mitochondria from these species were biofunctionally intact and structurally well-preserved. We then co-cultured Mito-Tracker Green-labeled mitochondria from these species with WGA594 red fluorescently-labeled human cardiomyocytes (AC16), human hepatocarcinoma cells (HepG2), and mouse skin fibroblasts (L929), observing efficient internalization and significant co-localization of the various mitochondria within recipient cells (Figure 1H).

To evaluate the safety of these interspecies mitochondrial transplants, we collected the supernatants of the co-cultured cells and assessed immune and inflammatory responses

using ELISA. We found no significant changes in the levels of IL-6, IL-10, and TNF-α in the mitochondria-transplanted groups compared to normal cells (Figures 1I-N), indicating a high degree of safety for multi-species mitochondrial transplantation.

Additionally, we included mitochondria from Vaucheria litorea, further pushing the species boundary. After labeling these mitochondria with Mito-Tracker Red and co-culturing them with WGA594-labeled L929 cells (Figures S1A-B), we observed that although most of the plant mitochondria were damaged due to extraction techniques, some intact ones were still internalized by the cells. Given the complexity of plant mitochondrial extraction and the significant genetic divergence between plant and animal mitochondria, the safety and efficacy of such transplants would substantially bolster our findings. We conducted Vaucheria litorea mitochondrial transplantation every three days for 25 days, initially observing immune responses in the first five transplants. However, starting from the sixth transplant, due to contamination and other factors, IL-6, IL-10, and TNF-α levels surged, leading to cell death (Figures S1C-F). While the outcome of plant mitochondrial transplantation is largely acceptable, as the extraction of plant mitochondria has a high contamination risk, the initial success of these transplants sufficiently demonstrated the universality and safety of mitochondrial transplantation. The internalization of mitochondria from multiple species reflects the cellular "inclusiveness" to various foreign organelles.

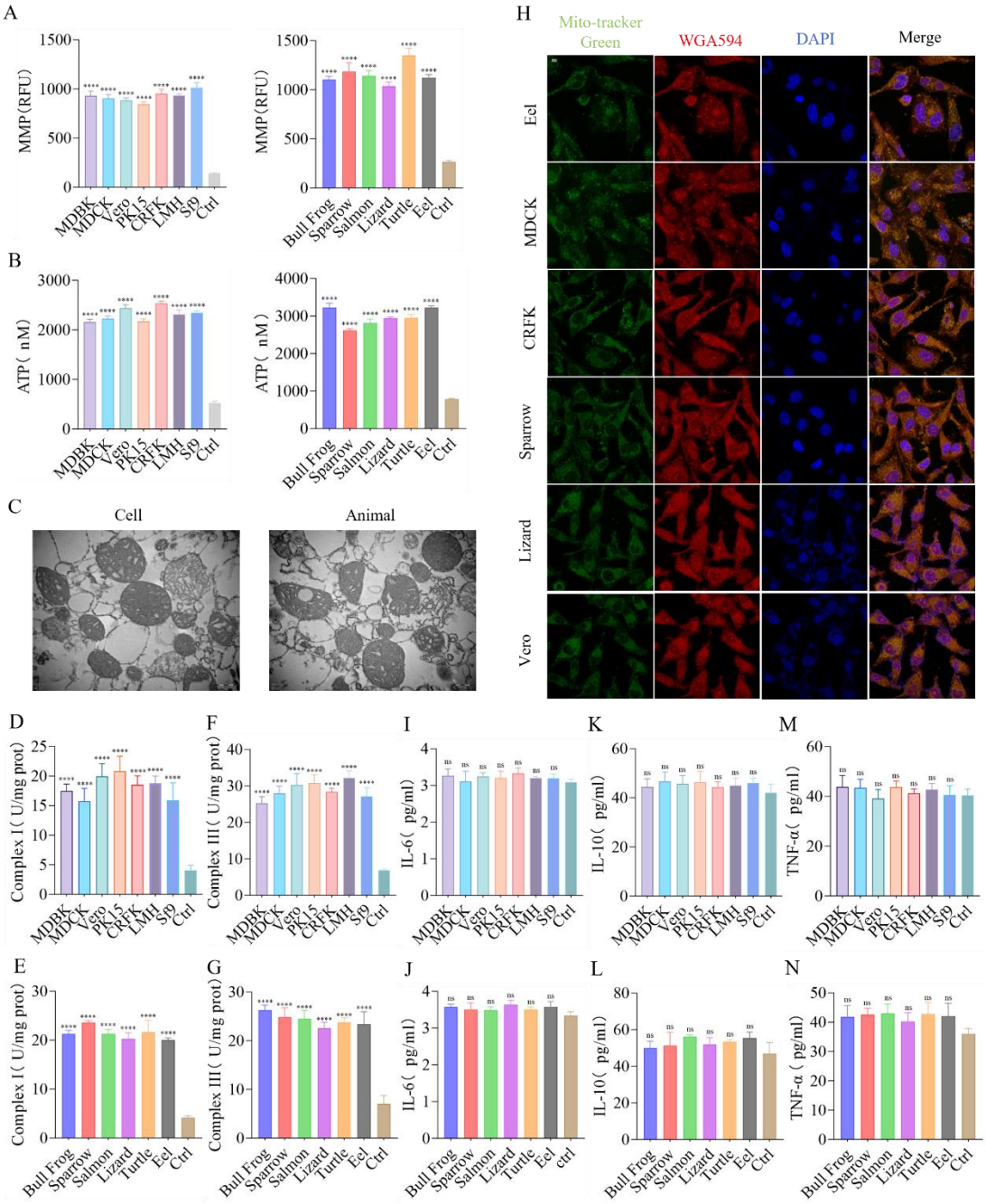

Figure 1: Universality of Mitochondrial Transplantation

(A) Analysis of membrane potential in both cells and animals isolated mitochondria. Ctrl: Mitochondria subjected to two freeze-thaw cycles at -80°C and 37°C to completely disrupt their structure and function, used for comparison.

(B) ATP production capacity in both cells and animals isolated mitochondria. Ctrl: Mitochondria subjected to two freeze-thaw cycles at -80°C and 37°C, used for comparison.

(C) Morphology of mitochondria from cells and animals observed under electron microscopy. Scale bar: 500 nm.

(D-G) Activity of respiratory chain complexes I and III in both cells and animals isolated mitochondria.
(H) Co-localization fluorescence imaging at 24 hours of transplanted mitochondria labeled with Mito-Tracker Green (green fluorescence) from Eel, MDCK, CRFK, Sparrow, Vero, and Lizard with AC16, L929, and HepG2 cells labeled with WGA594 (red fluorescence). Blue fluorescence DAPI represents the nucleus. Scale bar: 30 μm.
(I-N) Immunoreactivity of IL-6, IL-10, and TNF-α in cell culture medium collected 24 hours after the transplantation of exogenous mitochondria. Ctrl: Untreated group.
ns = no statistical significance, **** = $p<0.0001$.

Mitochondria with Matching Metabolic Characteristics Provide Better Therapeutic Outcomes

Eukaryotic mitochondria are maternally inherited. Although the gene sequence and composition are relatively conservative, their sequence variation rate is quite fast, which makes the mitochondrial genes differ in different species over a long period of evolution, that is to say, the mitochondria of various species are unique(Broughton & Reneau, 2006, Burki, 2016, Butenko, Lukeš et al., 2024, Gray, 2012, Gray et al., 1999, Logan, 2003, Mahler, 1981, Raval, Martin et al., 2023). Given the universality of mitochondrial transplantation and the ability to transplant mitochondria from various species, we explored whether the species-specific characteristics of mitochondria might lead to different therapeutic outcomes. Additionally, factors such as the physiological state of the donor organism, cell culture conditions, and mitochondrial isolation methods can influence mitochondrial function, raising questions about whether these differences affect therapeutic efficacy.

In organ and stem cell transplantation, metabolic compatibility is crucial for achieving optimal therapeutic outcomes, and mitochondrial transplantation is no exception(Broughton & Reneau, 2006, Levoux, Prola et al., 2021, Zhang, Liu et al., 2023). This raises the question: When mitochondrial functions are similar, do metabolically matched mitochondria offer better therapeutic outcomes? I hypothesized that, in the absence of significant functional differences, metabolically matched mitochondria would yield superior therapeutic effects. To minimize variables, we used mitochondria from four different kidney cell species and selected functionally similar mitochondria based on MMP and ATP assessments (Figures 2A, 2B, 2J, and 2K). We then co-cultured these mitochondria with cells under different disease model conditions, observing varying therapeutic effects.

In the H2O2-induced BMDM oxidative stress model(Jin, Wang et al., 2014), all mitochondrial transplant groups showed significant therapeutic effects, but the MDCK group notably enhanced cell viability compared to the MDBK and Vero groups (Figure 2C). Immunofluorescence staining revealed a marked reduction in mitochondrial ROS production in all transplant groups (Figure 2D), with a significant reduction of

mitochondrial ROS in the MDCK group compared to the MDBK group (Figure 2E). Additionally, lipid peroxidation was significantly decreased, and glutathione levels were notably increased in the MDCK group compared to the Vero group (Figures 2F-G). Overall, these results suggest that MDCK mitochondrial transplantation is more effective in treating H2O2-induced oxidative stress in BMDMs. Despite no significant differences in mitochondrial function among the groups based on ATP and MMP analysis, the MDCK group showed a slight advantage (Figures 2A-B). To exclude the impact of minor functional differences, we paired MDBK mitochondria with MDCK mitochondria and Vero mitochondria with PK15 mitochondria, labeling them with Mito-Tracker Deep-Red and Mito-Tracker Green, respectively. After co-culturing with H2O2-treated BMDMs for 24 hours, fluorescent immunostaining showed no significant competition between the different mitochondria, and their internalization levels were comparable (Figures 2H-I).

Since there were no significant functional differences among the four types of mitochondria and their internalization levels were similar, the only distinction was their species of origin. Although the primary function of mitochondria is to provide energy, their auxiliary functions, which vary among species, seem to have made the MDCK mitochondria more metabolically compatible with the H2O2-treated BMDMs, resulting in better therapeutic outcomes.

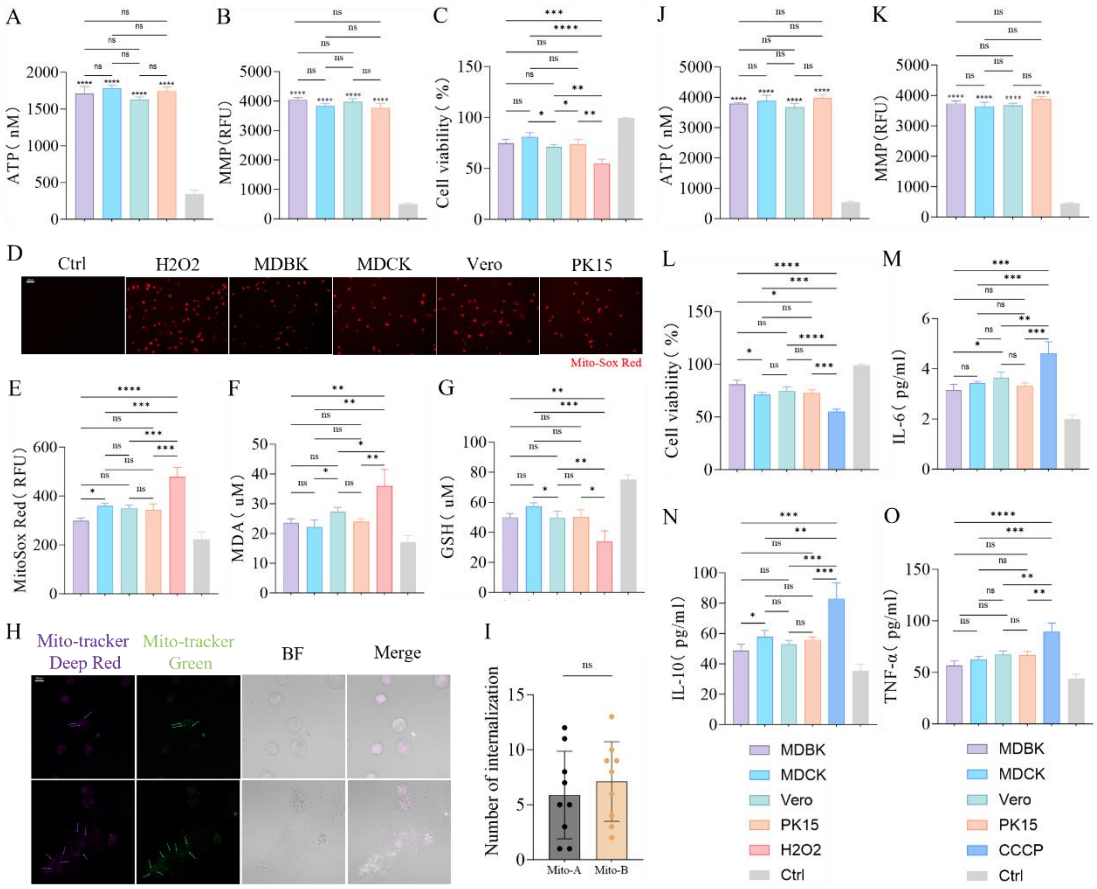

Figure 2: Mitochondria with Matching Metabolic Characteristics Provide Better Therapeutic Outcomes

(A, J) ATP production capacity in isolated mitochondria. Ctrl: Mitochondria subjected to two freeze-thaw cycles at -80°C and 37°C, used for comparison.

(B, K) Membrane potential in isolated mitochondria. Ctrl: Mitochondria subjected to two freeze-thaw cycles at -80°C and 37°C, used for comparison.

(C) Effects of mitochondria transplantation from four different species on the viability of BMDM cells after H2O2 treatment. Ctrl: Untreated group.

(D) Effects of mitochondria transplantation from four different species on reactive oxygen species (ROS) in BMDM cells after H2O2 treatment. Ctrl: Untreated group.

(E) Fluorescence imaging of mitochondrial ROS intensity in BMDM cells 24 hours after transplantation of mitochondria from four different species, followed by H2O2 treatment. Ctrl: Untreated group. Scale bar: 30 μm.

(F-G) Effects of mitochondria transplantation from four different species on MDA and GSH levels in BMDM cells after H2O2 treatment. Ctrl: Untreated group.

(H-I) Fluorescence imaging and statistical analysis of the internalization of mitochondria A labeled with Mito-Tracker Red (red fluorescence) and mitochondria B labeled with Mito-Tracker Green (green fluorescence) in BMDM cells after H2O2 treatment. Scale bar: 30 μm.

(L) Effects of mitochondria transplantation from four different species on the viability of HepG2 cells after LPS treatment. Ctrl: Untreated group.

(M-O) Changes in IL-6, IL-10, and TNF-α levels in HepG2 cells after LPS treatment, following mitochondria transplantation from four different species. Ctrl: Untreated group.

ns = no statistical significance, * = $p<0.05$, ** = $p<0.01$, *** = $p<0.001$, **** = $p<0.0001$.

In CCCP-treated AC16 cells(Ganote & Armstrong, 2003), despite similar mitochondrial function based on ATP and MMP assessments (Figures 2J-K), the MDBK group showed no significant advantage. Nevertheless, its therapeutic effect was superior, significantly enhancing cell viability compared to the MDCK and PK15 groups (Figure 2L). The MDBK group also had lower IL-6 levels compared to the Vero group (Figure 2M) and lower IL-10 levels compared to the MDCK group (Figure 2N), although there were no significant differences in TNF-α levels among the groups (Figure 2O). Overall, the MDBK mitochondria exhibited better anti-inflammatory effects in CCCP-treated AC16 cells. Despite the lack of functional advantages, the superior therapeutic outcomes in the MDBK group suggest that its mitochondria were more metabolically compatible with the CCCP-treated AC16 cells. These findings warrant further investigation.

We also extracted mitochondria from the four kidney cell species and co-cultured them with LPS-treated HepG2 cells(Fuchs, Radun et al., 2022). In this case, despite similar mitochondrial function across groups, the Vero mitochondria exhibited better therapeutic efficacy (Figures S4A-B), significantly enhancing cell viability compared to the MDCK and PK15 groups (Figure S4C). The Vero mitochondria also reduced mitochondrial ROS

production compared to the MDCK group (Figure S4D) and decreased IL-6 levels more effectively than the MDBK group (Figure S4E). Although IL-10 levels showed no significant differences among the groups, the Vero mitochondria still exhibited a slight advantage (Figure S4F). These results indicate that Vero mitochondria were more effective in treating LPS-induced stress in HepG2 cells, supporting my hypothesis that metabolic compatibility plays a critical role in the therapeutic effects of mitochondrial transplantation. However, the lack of expected results in IL-10 detection and the absence of significant differences in TNF-α levels in CCCP-treated AC16 cells suggest that the compatibility between mitochondrial characteristics and cellular metabolism might have limits. The therapeutic effects of mitochondrial transplantation are primarily reflected in their core functions, and these results may not scale significantly when translated from cell culture to animal models or human treatments. Therefore, further exploration of the potential to enhance mitochondrial transplantation by integrating the characteristics of multiple mitochondrial species is warranted.

Generation of More Potent Pluripotent Hybrid Mitochondria through Mitochondrial Fusion

Mitochondrial transplantation can endow recipient cells with the characteristics of donor mitochondria. For instance, co-culturing mitochondria from human mammary epithelial cells with breast cancer cells has been shown to inhibit glycolysis, reduce glucose uptake, suppress cancer cell proliferation, and enhance sensitivity to paclitaxel(Jiang et al., 2015). Similarly, co-culturing mitochondria containing antibiotic resistance genes with antibiotic-sensitive cells can improve resistance to antibiotics(Clark & Shay, 1982). Given that cell fusion can lead to metabolic reprogramming, enabling fused cells to acquire traits from different cell types(Song, Choi et al., 2022), a question arises: can mitochondria within fused cells also gain multi-lineage characteristics? Both current studies and my research indicate that mitochondria do not seem to have lineage restrictions, suggesting the potential to create mitochondria with enhanced characteristics through fusion. Could mitochondria with multi-lineage traits offer superior therapeutic efficacy under equivalent functional conditions?

I conducted a study in which HL1 and H9C2 cells were fused. The fusion cells were harvested and validated using immunofluorescence (Figure 3A) and flow cytometry (Figure 3B and Figures S2C-F), followed by passaging and subsequent co-culture with CCCP-induced mitochondrial damage in AC16 cells. Mitochondria were extracted from HL1, H9C2, and HL1+H9C2 fused cells and co-cultured with AC16 cells. MMP and ATP assays confirmed that all three groups had well-preserved mitochondrial function with no significant differences (Figures 3C-D). All groups significantly improved AC16 cell viability, with the HL1+H9C2 group showing the most pronounced effect (Figure 3E). Immunofluorescence analysis revealed that all mitochondrial transplantation groups

markedly reduced ROS production in the cells (Figure 3G), with quantitative fluorescence data indicating a significant reduction in mitochondrial ROS in the HL1+H9C2 group compared to the H9C2 group (Figure 3F). Although there was no significant difference in MDA levels among the three groups (Figure 3H), the GSH levels were significantly higher in the HL1+H9C2 group compared to the H9C2 group (Figure 3I). Overall, the HL1+H9C2 group demonstrated superior therapeutic effects on AC16 cells.

Although the therapeutic efficacy of hybrid mitochondria from fused cells was stronger than that of single-lineage mitochondria, the advantage was not substantial. HL1 and H9C2 cells are phylogenetically close, sharing similar lineage characteristics, which may explain the less pronounced therapeutic effect. Nevertheless, this finding aligns with the conclusion from the second section: mitochondria with better metabolic compatibility exhibit superior therapeutic effects when the mitochondrial biological functions are not much different.

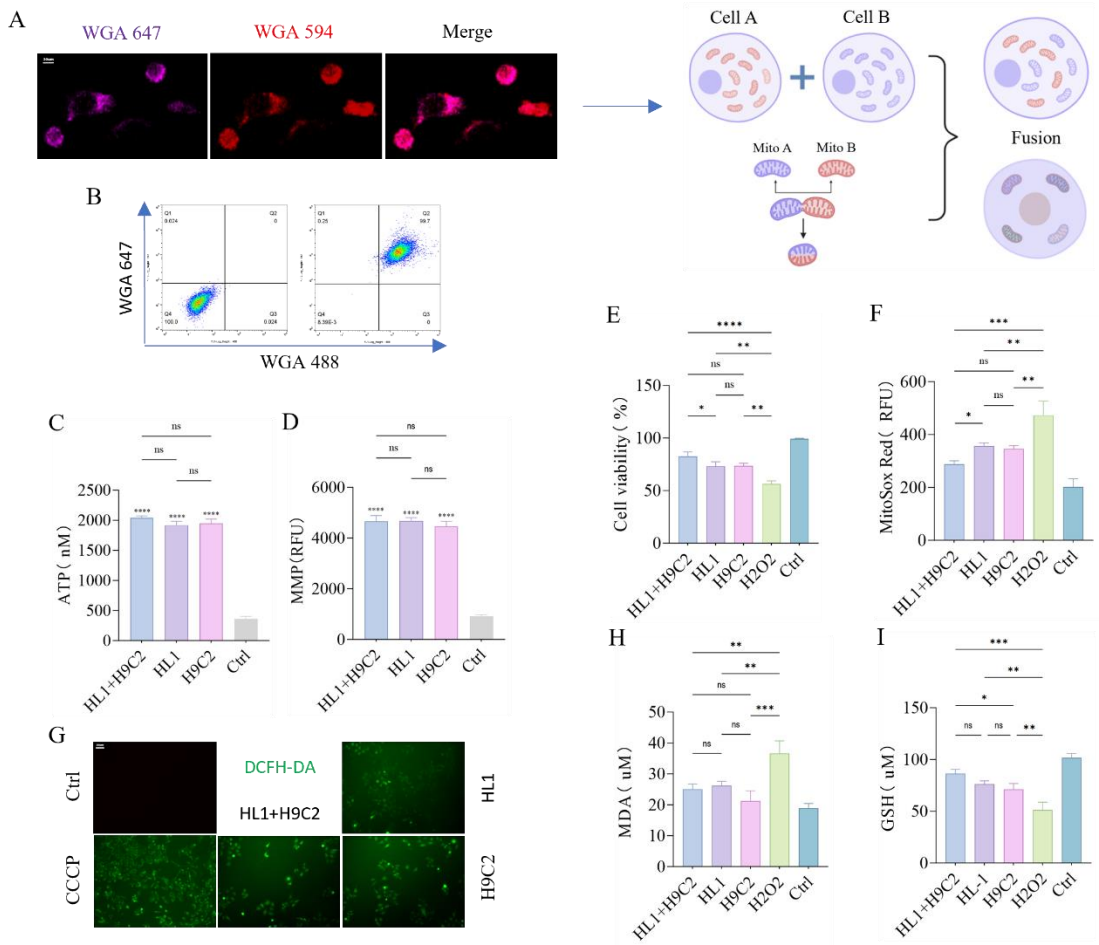

Figure 3: Generation of More Potent Pluripotent Hybrid Mitochondria through Mitochondrial Fusion

(A) Co-localization fluorescence imaging 24 hours after the fusion of HL1 cells labeled with WGA647 (deep red fluorescence) and H9C2 cells labeled with WGA594 (red fluorescence). Scale bar: 30 μm.

(B) Flow cytometric sorting of hybrid cells 24 hours after the fusion of HL1 cells labeled with WGA647 (deep red fluorescence) and H9C2 cells labeled with WGA488 (green fluorescence).

(C) ATP production capacity in isolated mitochondria, Ctrl: Mitochondria subjected to two freeze-thaw cycles at -80°C and 37°C, used for comparison.
(D) Membrane potential in isolated mitochondria, Ctrl: Mitochondria subjected to two freeze-thaw cycles at -80°C and 37°C, used for comparison.
(E) Effects of transplantation of three different types of mitochondria on the viability of AC16 cells after H2O2 treatment. Ctrl: Untreated group.
(F) Effects of transplantation of three different types of mitochondria on mitochondrial ROS levels in AC16 cells after H2O2 treatment. Ctrl: Untreated group.
(G) Changes in ROS levels in AC16 cells after H2O2 treatment, following transplantation of three different types of mitochondria. Ctrl: Untreated group. Scale bar: 30 μm.
(H-I) Effects of transplantation of mitochondria from four different species on MDA and GSH levels in AC16 cells after H2O2 treatment. Ctrl: Untreated group.
ns = no statistical significance, * = $p<0.05$, ** = $p<0.01$, *** = $p<0.001$, **** = $p<0.0001$

Competitive Internalization of Mitochondria: The Fittest Functions Best

Natural selection dictates that the fittest survive, a principle that also applies to mitochondrial transplantation(Reznick & Ricklefs, 2009). When the bioenergetic function of transplanted mitochondria varies significantly, the more suitable mitochondria may provide better therapeutic outcomes.

Given the variability in bioenergetic function due to differences in the physiological state and rearing environment of animals, I extracted mitochondria from the liver tissues of sparrows, lizards, salmon, and bullfrogs and co-cultured them with CCCP-treated HepG2 cells(Hsu, Wang et al., 2013). ATP and MMP assessments indicated that the mitochondria from bullfrogs exhibited the strongest bioenergetic function among the four groups (Figures 4A-B). All four types of mitochondria significantly restored mitochondrial membrane potential, demonstrating their therapeutic potential (Figure S3A). However, the bullfrog mitochondria significantly enhanced HepG2 cell viability compared to the sparrow and lizard mitochondria (Figure 4C). They also markedly reduced mitochondria ROS production compared to the sparrow and salmon groups (Figure 4D) and better repaired DNA oxidative damage than the other three groups (Figure 4E). Immunofluorescence further revealed that HepG2 cells internalized a greater quantity of bullfrog mitochondria compared to lizard mitochondria (Figures 4F-G). This suggests that while metabolic compatibility is important when bioenergetic function is similar, superior bioenergetic function provides better therapeutic effects when there is a significant difference.

I conducted a similar experiment by extracting mitochondria from the liver tissues of the four animals and co-culturing them with LPS-treated BMDM cells(Volchuk, Ye et al., 2020). ATP and MMP assessments showed that salmon mitochondria exhibited stronger

bioenergetic function than the others (Figures 4H-I). All four types of mitochondria effectively restored mitochondrial membrane potential in LPS-treated BMDM cells (Figure S3B). However, bullfrog mitochondria showed a more significant therapeutic effect by enhancing cell viability and reducing inflammation and DNA oxidative damage compared to the other groups. Bullfrog mitochondria significantly improved cell viability compared to the other three groups (Figure 4J), reduced IL-6 levels compared to the salmon and lizard groups (Figure 4K), lowered TNF-α levels compared to the other three groups (Figure 4L), and decreased IL-10 levels compared to the sparrow and salmon groups (Figure 4M). They also reduced 8-OHDG levels more than other three groups (Figure 4N). Immunofluorescence analysis revealed that bullfrog mitochondria were internalized at a much higher rate than lizard and sparrow mitochondria (Figures 4O-P). These results indicate that, under equal conditions, cells actively select mitochondria that are more beneficial to them, while mitochondria compete to out-survive each other, demonstrating the classic law of "survival of the fittest." Moreover, I cultured P5 generation PK15, P15 generation MDBK, P15 generation MDCK, P15 generation Vero to create mitochondria with varying bioenergetic strengths and co-cultured them with H2O2-treated HepG2 cells(Hu, Lu et al., 2022). ATP and MMP assessments revealed that mitochondria from early-passage PK15 cells exhibited stronger bioenergetic function than those from MDBK and Vero cells (Figures S4G-H). PK15 mitochondria significantly improved HepG2 cell viability (Figure S4I) and reduced ROS production (Figure S4J) compared to MDBK and MDCK cells. They also increased GSH levels (Figure S4K) and decreased MDA production more than MDCK mitochondria (Figure S4L), reducing oxidative stress in HepG2 cells, further confirming the therapeutic advantage of mitochondria with stronger bioenergetic function.

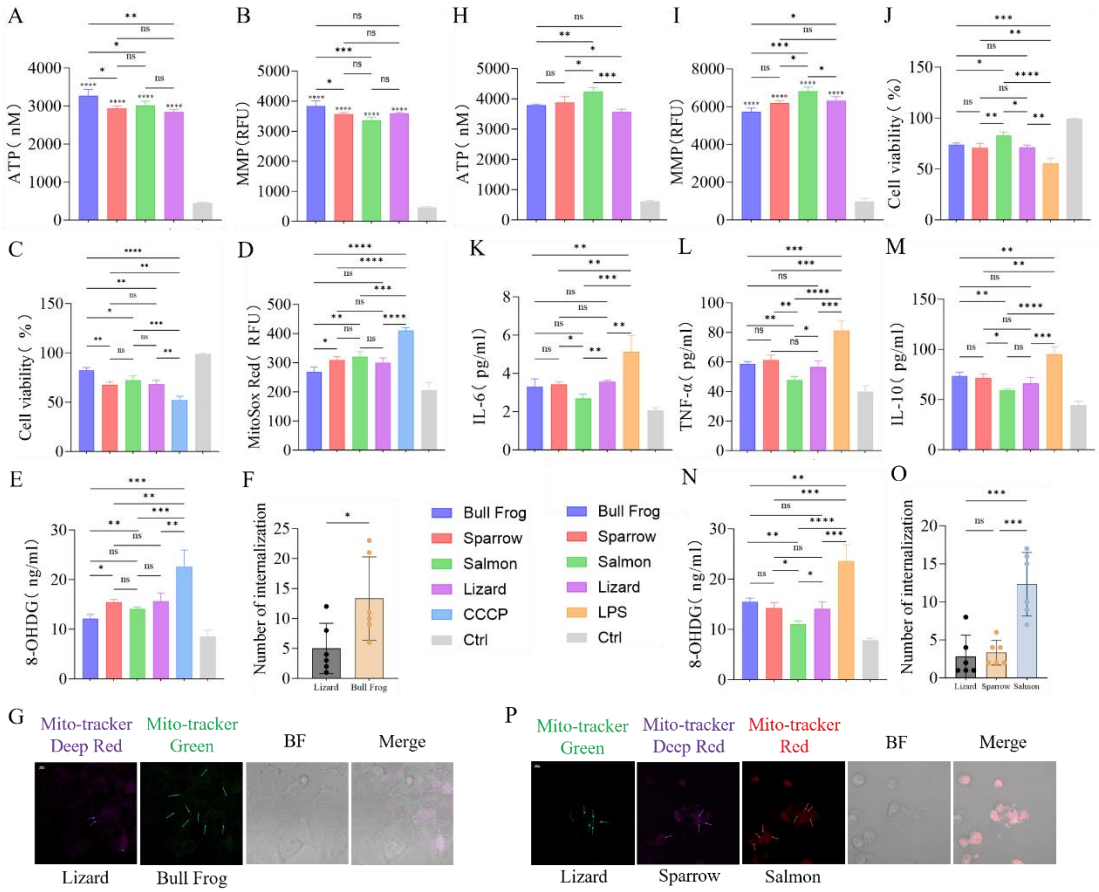

Figure 4: Competitive Internalization of Mitochondria: The Fittest Functions Best

(A, H) ATP production capacity in isolated mitochondria. Ctrl: Mitochondria subjected to two freeze-thaw cycles at -80°C and 37°C, used for comparison.

(B, I) Membrane potential in isolated mitochondria. Ctrl: Mitochondria subjected to two freeze-thaw cycles at -80°C and 37°C, used for comparison.

(C) Effects of mitochondria transplantation from four different species on the viability of HepG2 cells after CCCP treatment. Ctrl: Untreated group.

(D) Effects of mitochondria transplantation from four different species on mitochondria ROS in HepG2 cells after CCCP treatment. Ctrl: Untreated group.

(E) Detection of DNA damage repair in HepG2 cells after CCCP treatment following mitochondria transplantation from four different species. Ctrl: Untreated group.

(F-G) Fluorescence imaging and statistical analysis of the internalization of Lizard mitochondria labeled with Mito-Tracker Deep-Red (deep red fluorescence) and Bull Frog mitochondria labeled with Mito-Tracker Green (green fluorescence) in HepG2 cells after CCCP treatment. Scale bar: 30 μm.

(J) Effects of mitochondria transplantation from four different species on the viability of BMDM cells after LPS treatment. Ctrl: Untreated group.

(K-M) Changes in IL-6, IL-10, and TNF-α levels in BMDM cells after LPS treatment following mitochondria transplantation from four different species. Ctrl: Untreated group.

(N) Detection of DNA damage repair in BMDM cells after LPS treatment following mitochondria

transplantation from four different species.
(O-P) Fluorescence imaging and statistical analysis of the internalization of Lizard mitochondria labeled with Mito-Tracker Green (green fluorescence), Sparrow mitochondria labeled with Mito-Tracker Deep-Red (deep red fluorescence), and Salmon mitochondria labeled with Mito-Tracker Red (red fluorescence) in HepG2 cells after CCCP treatment. Scale bar: 30 μm.
ns = no statistical significance, * = $p<0.05$, ** = $p<0.01$, *** = $p<0.001$, **** = $p<0.0001$

The internalization of plant mitochondria also reflects this result. Due to the variability in mitochondrial quality upon extraction, they were categorized into three groups: mostly dead, partially functional, and a small portion that was fully functional (Figure S1C). For normal L929 cells, the dead and partially functional mitochondria were excluded, and only the fully functional ones were internalized (Figure S1A). However, in L929 cells with mitochondrial and cellular damage, the range of internalization included both partially functional and fully functional mitochondria (Figure S1B). The differential internalization of mitochondria based on cellular and mitochondrial function suggests a form of mutual selection, reflecting the law of "survival of the fittest," where the mitochondria with stronger bioenergetic function are more likely to be internalized and survive.

Mitochondrial Transplantation Enhances Physical Function and Biological Potency in Mice

Mitochondrial transplantation temporarily supplements or replaces the mitochondria of recipient cells in the short term. However, the long-term biological outcome involves the bi-fusion and fission of both exogenous and endogenous mitochondria, leading to the formation of new mitochondria. Without continuous supplementation, exogenous mitochondria are eventually assimilated by the recipient cells, causing alterations in the metabolome, proteome, and even genome of the recipient cells(Doulamis, Nomoto et al., 2022, McCully, Del Nido et al., 2023, Tripathi & Ben-Shachar, 2024). However, as the fusion and fission cycles continue, similar to Mendelian inheritance, the influence of the foreign mitochondria diminishes over time, and the benefits they confer gradually fade(Hong, Kim et al., 2023, La Morgia, Maresca et al., 2020, Nitsch, Lareau et al., 2024). My in vitro experiments focus on demonstrating the impact of mitochondrial functionality on the efficacy of disease treatment. Only when the potent therapeutic effects of mitochondrial function are established do the germline characteristics and metabolic matching of mitochondria gain significance. Therefore, my in vivo experiments are limited to verifying the short-term therapeutic effects of mitochondrial transplantation on recipient cell function. We need to understand the limits of mitochondrial transplantation to lay the foundation for subsequent germline studies.

Our in vitro experiments indicate that mitochondria with greater functional potency exhibit superior therapeutic effects on diseases compared to mitochondria with normal function.

Is this also applicable in vivo? Studies suggest that preemptive administration of normally functioning mitochondria can enhance cellular resistance to stimuli(Ali Pour et al., 2020), but does this confer greater benefits to general recipients? Mitochondrial biogenesis, enhanced through training, increases mitochondrial function. Mice with trained mitochondria should, therefore, exhibit better therapeutic outcomes than those with autologous or allogeneic mitochondria with normal function(Shang, Bian et al., 2023, Souza-Tavares, Santana-Oliveira et al., 2024). The functional enhancement of mitochondria in trained mice is based on their overall physical fitness. Wild-type mice, being more robust with stronger metabolism, are hypothesized to possess even more potent mitochondrial function.

Using a D-gal-induced aging mouse model(Jiang, Ji et al., 2023), we extracted mitochondria from mouse myoblasts (C2C12), young C57B/L 6J(4 months old) gastrocnemius muscle tissue, HIIT-trained C57B/L 6J gastrocnemius muscle, HIIT-trained human gastrocnemius muscle, and wild mouse gastrocnemius muscle for tail vein injection into aged mice, subsequently, mitochondria from the gastrocnemius muscle tissue of HIIT-trained C57B/L6J mice and wild mice were selected for intravenous tail injection into 4-month-old normal C57B/L6J mice. Additionally, we co-cultured mitochondria from each group with normal HepG2 and D-gal-treated HepG2 cells.

ATP and MMP assessments revealed significant differences in mitochondrial function between the Wild Mice group and the C2C12, Young C57, and Trained People groups. There was also a significant difference between the Trained C57 and Young C57 groups, with the Wild Mice group showing a slight advantage over the Trained C57 group, though not statistically significant (Figures 5A-B). No immune inflammatory response was observed 24 hours post-surgery (Figure S5A). In the aging model, all groups showed improved exercise performance three days post-transplantation, with the Wild Mice and Trained C57 groups demonstrating greater endurance (Figure 5C). In the normal model, only the Wild Mice group showed improved endurance (Figure 5I). One week post-transplantation, body weight significantly increased in all aging model groups, with the Wild Mice group showing the greatest recovery (Figure 5D-E). No significant differences were observed in the normal model groups (Figures 5J-K). Although all transplant groups had therapeutic effects, the Wild Mice group more significantly reduced oxidative stress in aged mice, showing lower MDA levels compared to the Young C57 and Trained People groups (Figure 5F). NOS levels were lower in the Wild Mice group compared to the C2C12, Young C57, and Trained People groups; although the Trained C57 group also differed significantly from the Young C57 group, it was still inferior to the Wild Mice group (Figure 5G). The Wild Mice group had significantly higher SOD activity compared to the C2C12, Young C57, and Trained C57 groups and also increased SOD activity in normal mice (Figures 5H and 5M). Furthermore, mitochondrial transplantation increased the bioenergetic capacity of normal L929 cells, with the Wild Mice and Trained C57 groups

showing the greatest enhancement, particularly the Wild Mice group (Figure 5O). All mitochondrial transplant groups partially restored MMP in CCCP-treated L929 cells, significantly reducing ROS production. The Wild Mice and Trained C57 groups had better MMP recovery, more normal mitochondrial morphology, and lower ROS fluorescence intensity (Figures 6A-B). Ranking mitochondrial function suggests Wild Mice > Trained C57 > Young C57 ≈ Trained People ≈ C2C12. The observed therapeutic effects support the conclusion that mitochondria with greater functional potency provide better therapeutic outcomes, establishing a positive correlation. Given the robust physical fitness of wild animals, their mitochondria might currently be the most potent. I believe that mitochondrial transplantation has no upper limit but only continues to yield better therapeutic results, which applies to general recipients as well.

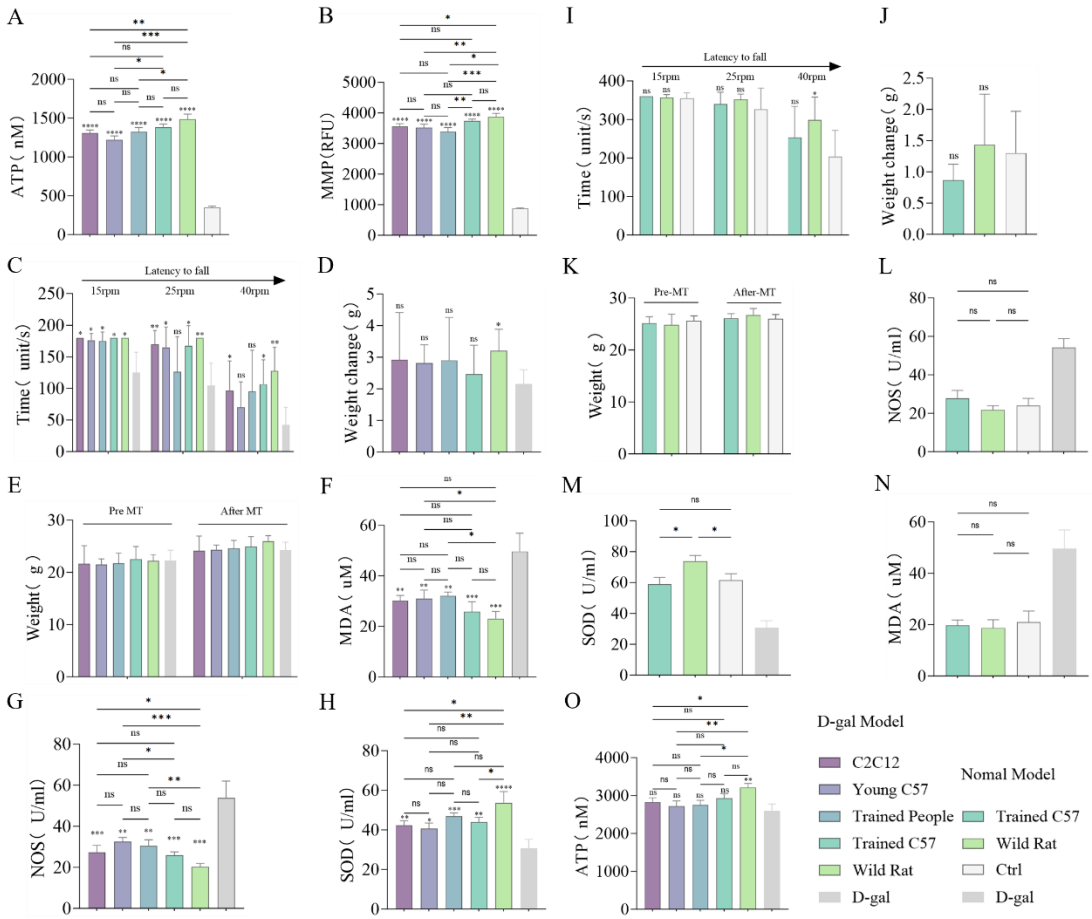

Figure 5: Mitochondrial Transplantation Enhances Physical Function and Biological Potency in Mice

(A-B) Measurement of ATP production capacity and membrane potential in isolated mitochondria. Ctrl: Mitochondria subjected to two freeze-thaw cycles at -80°C and 37°C, used for comparison.

(C) Changes in body weight of D-gal model mice following transplantation of five different types of mitochondria. (D) Changes in motor ability of D-gal model mice following transplantation of five different types of mitochondria. (E-G) Evaluation of the antioxidant and oxidative capacity of D-gal model mice by measuring serum glutathione content, superoxide dismutase activity, and malondialdehyde levels after

transplantation of five different types of mitochondria.

(H) Changes in body weight of normal mice after transplantation of two different types of mitochondria. Ctrl: Untreated group.

(I) Effects of transplantation of two different types of mitochondria on the motor ability of normal mice. Ctrl: Untreated group.

(J-L) Evaluation of the antioxidant and oxidative capacity of normal mice by measuring serum GSH content, SOD activity, and MDA levels after transplantation of two different types of mitochondria. Ctrl: Untreated group.

(M) Changes in ATP production capacity in normal HepG2 cells after transplantation of five different types of mitochondria. Ctrl: Untreated group.

ns = no statistical significance, * = $p<0.05$, ** = $p<0.01$, *** = $p<0.001$, **** = $p<0.0001$

Unfortunately, due to the poor efficacy of D-gal, the two-month treatment failed to adequately reproduce the aging mouse model, resulting in limited experimentation. Consequently, we conducted a second animal experiment, isolating mitochondria from the gastrocnemius muscles of Young C57B/L 6J (4 months old) and Wild Mice for tail vein injection into both acute inflammation mouse model(Fu, Liu et al., 2015) and normal mouse model. We also co-cultured mitochondria from each group with normal and LPS-treated BMDM. ATP and MMP analyses showed that Wild Mice mitochondria had the highest functional potency (Figures 6C-D), with no immune inflammatory response observed after 24 hours (Figure S5B). Small animal imaging detected the absorption of exogenous mitochondria by severely damaged liver and kidney tissues via the circulatory system (Figure 6E). Three days post-transplantation, grip strength and endurance were significantly restored in all acute inflammation model groups, with the Wild Mice group showing the most notable endurance improvement (Figures 6F and 6J). No significant differences in grip strength were observed in the Normal C57 groups, but the Wild Mice group had significantly improved endurance compared to the Ctrl group (Figures 6F and 6K). After one week, body weight had recovered in all acute inflammation model groups, with the Wild Mice group showing a significant increase compared to the LPS group (Figure 6H). No significant differences in body weight were observed in the normal mouse groups (Figure 6I). MRI assessment indicated significant increases in hind limb muscle volume in both the Wild Mice and Young C57 groups in the acute inflammation model, with the Wild Mice group slightly outperforming the Young C57 group (Figures S5D and 5E). Muscle tissue damage recovery was also better in the Wild Mice group (Figures S5D and 5F). Serum levels of IL-6, IL-10, and TNF-α were reduced in both the Wild Mice and Young C57 groups after treatment, with the Wild Mice group showing lower levels of IL-10 and TNF-α compared to the Young C57 group, and no significant changes were observed in the normal mouse groups (Figures 7A-C). Liver and kidney function were significantly improved in the Wild Mice and Young C57 groups, with serum AST levels significantly lower in the Wild Mice group compared to the Young C57 group. No significant differences were observed in the Normal C57 groups (Figures 7D-F). Both the

Wild Mice and Young C57 groups significantly reduced oxidative stress in the acute inflammation model, with lower MDA levels and higher SOD activity in the Wild Mice group compared to the Young C57 group. The Wild Mice group also significantly increased SOD activity in normal mice, although there was no difference in MDA levels among the groups (Figures 7G-H). Expression of inflammatory proteins in the liver and kidney tissues was reduced in both the Wild Mice and Young C57 groups in the acute inflammation model, with the Wild Mice group showing lower P-JNK protein expression compared to the Young C57 group (Figures 7I-K). Real-time quantitative PCR showed downregulation of IL-6, IL-8, IL-18, TGF-β, MPO, CXCL1, CXCL2, and HMGB1 and upregulation of IL-13, SOD1, ARG1, and COX1 in the kidneys of the Wild Mice and Young C57 groups compared to the LPS group. In the liver, IL-6, IL-8, IL-18, IL-1β, CXCL2, CCL5, CCL10, and TGF-β were downregulated, while IL-4, IL-13, ARG1, and SOD1 were upregulated (Figures S5G-H), with significant differences between the Wild Mice and Young C57 groups, indicating the superior therapeutic effect of Wild Mice mitochondria.

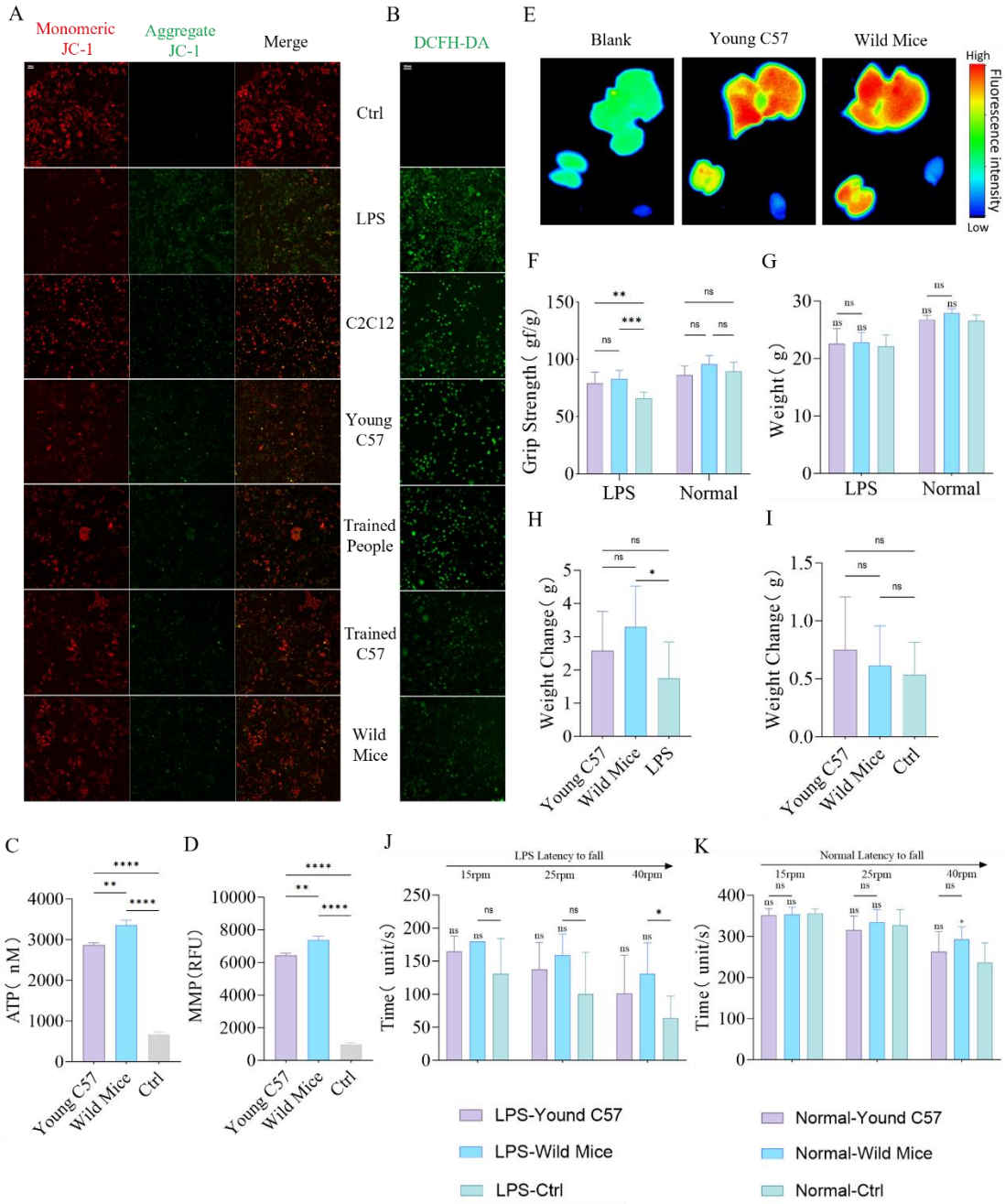

Figure 6: Mitochondrial Transplantation Enhances Physical Function and Biological Potency in Mice

(A) Fluorescence imaging of mitochondrial membrane potential in HepG2 cells treated with CCCP 24 hours after transplantation of five different mitochondria, with untreated cells as control. Scale bar: 30 μm.

(B) Fluorescence imaging of reactive oxygen species (ROS) in HepG2 cells treated with CCCP after transplantation of five different mitochondria, with untreated cells as control. Scale bar: 30 μm.

(C-D) Evaluation of isolated mitochondria functions via ATP production and mitochondrial membrane potential (MMP) assays, with mitochondria subjected to two freeze-thaw cycles at -80°C and 37°C to completely disrupt structure and function as control.

(E) Biodistribution of exogenous mitochondria in mouse liver, kidney, and heart detected by in vivo imaging

24 hours after intravenous tail vein injection of mitochondria. Blank : untreated LPS model group mice.

(F-H) Body weight changes in acute inflammation model mice and normal mice before and one week after transplantation of two different mitochondria, with untreated groups as control.

(I) Grip strength measurement in acute inflammation model mice and normal mice three days after transplantation of two different mitochondria, with untreated groups as control.

(J-K) Motor function assessment in acute inflammation model mice and normal mice three days after transplantation of two different mitochondria, with untreated groups as control.

ns = no statistical significance, * = $p<0.05$, ** = $p<0.01$, *** = $p<0.001$, **** = $p<0.0001$

Co-culturing mitochondria from each group with normal BMDM enhanced their bioenergetic capacity, with the Wild Mice group showing the most significant ATP increase (Figure S5C). Both mitochondrial types improved cell viability in LPS-treated BMDM (Figure 7L) and reduced mitochondrial ROS production (Figure 7M-N), with the Wild Mice group demonstrating better oxidative stress relief and cell viability enhancement. The second animal experiment provided a more comprehensive validation. While the Young C57 group showed good results, the Wild Mice group exhibited superior therapeutic effects in the acute inflammation model and LPS-treated BMDM, further enhancing cellular bioenergetics and demonstrating the potential of mitochondrial transplantation in boosting biological function.

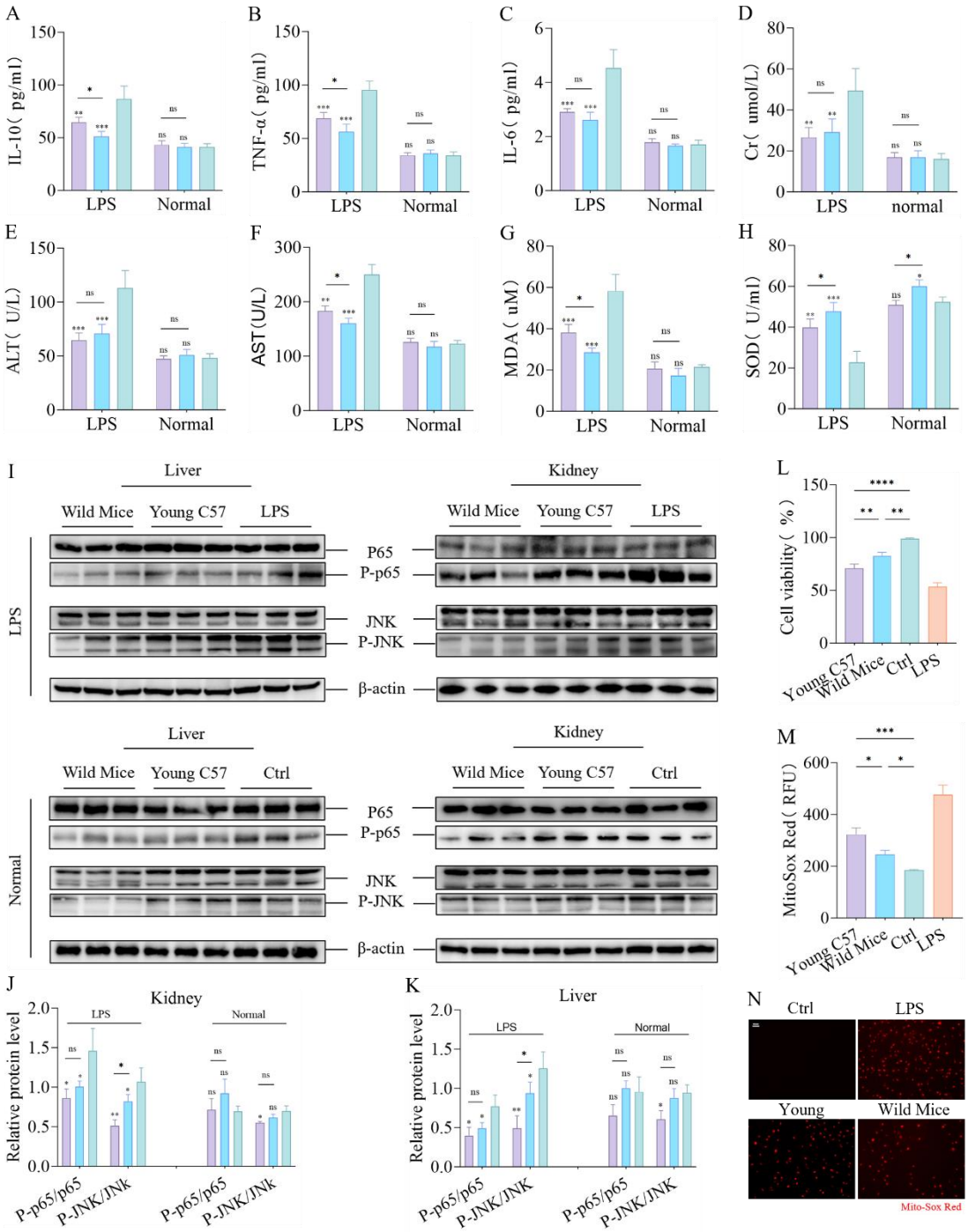

Figure 7: Mitochondrial Transplantation Enhances Physical Function and Biological Potency in Mice

(A-C) Changes in serum levels of IL-6, TNF-α, and IL-10 in acute inflammation model mice and normal mice one week after transplantation of two different mitochondria, with untreated groups as control.

(D-F) Evaluation of kidney and liver function via serum Cr, ALT, and AST levels in acute inflammation model mice and normal mice one week after transplantation of two different mitochondria, with untreated groups as control.

(G-H) Measurement of serum MDA levels and SOD activity in acute inflammation model mice and normal

mice one week after transplantation of two different mitochondria, with untreated groups as control.

(I-K) Analysis of JNK and P-JNK, p65, and P-p65 protein expression levels in liver and kidney tissues via Western blot one week after transplantation of two different mitochondria in acute inflammation model mice and normal mice, with untreated groups as control.

(L) Effects of two different mitochondria on the viability of LPS-treated BMDM cells 24 hours after transplantation, with untreated groups as control.

(M-N) Fluorescence imaging and quantitative analysis of mitochondrial ROS levels in LPS-treated BMDM cells 24 hours after transplantation of two different mitochondria, with untreated groups as control. Scale bar: 30 μm.

ns = no statistical significance, * = $p<0.05$, ** = $p<0.01$, *** = $p<0.001$, **** = $p<0.0001$

Discussion

The endosymbiotic nature of mitochondria grants them a unique non-immunogenic profile. The adaptation of organisms to their environments has resulted in mitochondria with unique functions, such as cytoplasmic male sterility in plants and drug resistance in eukaryotic cells, both of which are associated with mtDNA. Some mitochondrial functions remain unexplained, yet this does not hinder our exploration of mitochondrial transplantation(Cohen, Lobritz et al., 2013, Jin, Jiang et al., 2022, Lelandais, Albert et al., 1998). Transplanted mitochondria need to be metabolically compatible with recipient cells. If recipient cells acquire exogenous mitochondria with lineage-specific characteristics that match their metabolism and can adapt to different stimuli, could we harness different functions from mitochondria of various lineages? Could we, by extension, fuse and absorb unique functions from diverse organisms to accelerate evolution? Given that cells develop tolerance to various stimuli and drugs, could mitochondrial transplantation also develop tolerance? Repeated transplantation of the same type of mitochondria may gradually diminish its effects. Could we, therefore, obtain more potent mitochondria to avoid tolerance and allow the recipient to gradually adapt and enhance biological functions?

Therefore, I designed a series of experiments. The successful internalization of 14 different biological mitochondria by 3 types of cells, compared to previous studies, further confirms the universality and safety of mitochondrial transplantation, while expanding the sources of mitochondria. I hope this can provide patients with more diverse options. I further used 3 cell types and 4 disease models in various combinations to explore the possibility of merging mitochondrial characteristics from different sources. It appears that the source of mitochondria is not significantly restricted, allowing us to screen for mitochondria from different species that are more metabolically compatible and suitable for disease treatment. Since we can assimilate the characteristics of one type of mitochondria, we might also be able to assimilate the characteristics of multiple types. The hybrid mitochondria from HL1 and H9C2 lines exhibited stronger therapeutic effects compared to either HL1 or H9C2 alone, suggesting that it might be possible to artificially create such hybrid mitochondria

to target specific diseases. For example, mitochondria from scavengers like Komodo dragons and vultures might have enhanced antibacterial capabilities, while those from honey badgers or mongoose could possess better anti-venom properties. We could potentially combine these characteristics for targeted therapies, or even create multi-species hybrid mitochondria similar to multi-drug-resistant bacteria as a universal therapeutic approach. However, these approaches are based on the premise that the functional differences between the mitochondria used are not significant. For the average patient, single-lineage mitochondrial matching might be more appropriate due to safety concerns. As we aim to explore the potential of mitochondrial transplantation and find better therapeutic methods, I have further demonstrated the significant advantages of powerful mitochondria over metabolic matching in mitochondrial transplantation. These results suggest that the primary therapeutic effect of mitochondrial transplantation may be more related to the rescue of bioenergetics, with changes in cellular metabolism and proteomics being secondary.

We did not perform mitochondrial transplantation on the same batch of cells under different stimuli because the biological function of mitochondria is more critical than metabolic matching. Future research should focus on identifying more potent mitochondria for therapeutic applications. Although metabolic matching is currently important, especially from a safety perspective, it can serve as a foundation for mitochondrial fusion experiments to explore diverse biological therapies. In an artificially cultured environment, especially in stem cells where mitochondrial DNA oxidative damage accumulates less, the significant functional advantages of potent mitochondria may outweigh this benefit. While stem cells are a suitable source due to safety considerations, I believe that future mitochondrial transplantation would be more effective when based on a background of multiple germline sources, optimizing treatment options for metabolic matching. I cannot guarantee the absolute correctness of the current experiments, as the cumulative quantitative changes from multi-lineage hybrid mitochondrial transplantation might surpass the benefits brought by mitochondrial quality itself. Even now, I wouldn't claim that my research is entirely accurate; my experiments emphasize the possibilities of the future, particularly the potential for bio-enhancement.

The results of animal experiments were largely consistent with those of cell experiments, where mitochondria with various functional strengths demonstrated significant therapeutic effects. Notably, Wild Mice mitochondria were more effective in disease model mice and cells compared to other mitochondria. Although the Trained C57 mitochondria did not exhibit the same pronounced therapeutic effects as Wild Mice, their overall therapeutic enhancement was superior to other groups. The Trained People mitochondria did not show the expected therapeutic outcomes, which I attribute to my own suboptimal health due to prolonged lab work, leading to a slightly weaker enhancement of mitochondrial function compared to Trained C57. However, neither Young C57 nor Trained People mitochondria

showed a significant difference in therapeutic effect compared to C2C12, suggesting that in vivo mitochondria might compensate for the lower therapeutic efficacy associated with lower DNA oxidative damage in cellular mitochondria. We also observed an enhancement in the biological functions of normal cells by Wild Mice mitochondria, even improving the physiological functions of normal mice to some extent. Additionally, in these two mitochondrial transplantation pre-treatment cell experiments, we observed an increase in recipient cell ATP energy as mitochondrial function improved. This suggests a new solution to mitochondrial transplantation tolerance and potentially an optimized approach for multiple mitochondrial transplants. Importantly, our current results do not indicate a limit to the therapeutic effects of mitochondrial transplantation, implying that we can continue to explore more powerful mitochondria to better assist in treatment, and potentially even enhance human biological functions to some extent. This represents a significant expansion of the implications of mitochondrial transplantation, and I believe that my research could provide stronger and more diverse therapeutic options for clinical applications.

★STAR METHODS

Key Resources Table（See Appendix Key Resources Table）

Resource Availability

Lead Contact

Further information and requests for resources and reagents should be directed and will be fulfilled by the Lead Contact, Xiaomeng Lu（fylxmgg@gmail.com）.

Materials Availability

This study did not generate new unique reagents.

Data and Code Availability

This study did not generate datasets or code.

EXPERIMENTAL MODEL AND SUBJECT DETAILS

Cell Lines

Bovine kidney cells, porcine kidney cells, African green monkey kidney cells, feline kidney cells, canine kidney cells, human cardiomyocytes, rat cardiomyocytes, mouse cardiomyocytes, and human hepatocellular carcinoma cells were obtained from the Cell Center of the Chinese Academy of Sciences (China). Chicken hepatocellular carcinoma cells were purchased from Sunncell (China), and Spodoptera frugiperda cells and mouse fibroblasts were purchased from Procell (China). The bovine kidney cells, porcine kidney

cells, African green monkey kidney cells, feline kidney cells, canine kidney cells, chicken hepatocellular carcinoma cells, human cardiomyocytes, rat cardiomyocytes, mouse cardiomyocytes, mouse myoblasts, and human hepatocellular carcinoma cells were cultured in DMEM (Gibco) supplemented with 10% (v/v) fetal bovine serum (Gibco) and 1% (v/v) penicillin-streptomycin (Gibco) and incubated at 37°C in a humidified atmosphere with 5% CO2. Spodoptera frugiperda cells were cultured in SF-900TM II SEM (Gibco) medium in a shaker flask at 28°C.

Animals

The animal experiments involved in this study were all C57 B/L 6J strains purchased from the Animal Protection Center of Southern Medical University. All mice were maintained in a specific pathogen-free SPF environment. All mice were used in accordance with the scheme approved by the Review Committee of Southern Medical University. The mouse experimental scheme has been approved by the Animal Care and Use Committee of Southern Medical University, and the experimental animal facilities have been licensed by the Guangdong Medical Experimental Animal Center (SCXK-2021-0041). Lizards, salmon, bullfrogs, parakeets, turtles, and eels were purchased from animal breeding markets. Wild mice were captured using traps in the wild, disinfected, and then housed in the laboratory under appropriate conditions.

Human Subjects

The human subject involved in this study was the author. Full informed consent was obtained, and muscle tissue was surgically collected from the gastrocnemius muscle following ethical guidelines approved by the Ethics Review Board of Southern Medical University.

Plants

Vaucheria litorea was collected and transported under expert supervision and used immediately after thorough disinfection.

Isolation of Mouse Bone Marrow-Derived Macrophages (BMDMs)

Bones were aseptically harvested from the hind legs of C57BL/6 mice, and muscle tissues were removed. Bone marrow was flushed out of the bones using a 25-gauge needle attached to a syringe containing BMDM growth medium, which consists of DMEM, 20% L929 cell-conditioned medium to generate M-CSF, 10% FBS, and 1% penicillin/streptomycin. BMDMs were allowed to differentiate for 7 days at 37°C with 5% CO2, with the growth medium changed every 2 days during ex vivo culture.

Establishment of Cell Disease Models

Oxidative stress models were established by treating AC16 with 500 μM H2O2 for 24 hours and HepG2 cells with 700 μM H2O2 for 24 hours. Inflammation models were

established by treating BMDM cells with 100nM LPS for 24 hours and HepG2 cells with 1 μM LPS for 24 hours. Mitophagy models were established by treating AC16 and HepG2 cells with 30 μM CCCP for 24 hours. Senescence model was established by treating HepG2 cells with 30 g/L D-gal for 48 hours.

Disinfection and Sterilization of Plant Mitochondria

Weigh 1g of tissue and rinse with clean water for 3 hours. Transfer to a laminar flow hood, soak in 75% ethanol for 1 minute, then wash twice with DPBS containing 1% streptomycin/penicillin. After soaking in 2% NaClO for 8 minutes, wash three times with DPBS containing 1% streptomycin/penicillin for 1 minute each time. Then, rinse repeatedly in 1% $MgCL_2$ solution for 10 minutes. After that, wash three times with DPBS containing 1% streptomycin/penicillin. Place the sterilized tissue blocks into a 100mm² culture dish (Corning) and cut them into 0.1cm² pieces for further use.

Mitochondrial Isolation

Mitochondria were isolated from cultured cells, animal tissues, and plant tissues using the Mitochondria-Cytosol Protein Isolation Kit (C0010-50, Applygen) and the Plant Mitochondrial Extraction Kit (SM0020, Solarbio). For tissue homogenization, 100–200 mg of fresh animal tissue or 1 g of plant tissue was cut into 0.5 cm² pieces and placed into a Teflon-glass homogenizer with 2.5 ml of ice-cold mitochondrial extraction buffer. The tissue was homogenized 20 times using a tight-fitting pestle. For cell homogenization, 2-5 × 10^7 cells were collected, digested, centrifuged, washed, and resuspended in 1.5 ml of ice-cold mitochondrial extraction buffer. The cell suspension was transferred to a small glass homogenizer and homogenized 30 times using a tight-fitting pestle. The homogenate was transferred to a centrifuge tube and centrifuged at 800 × g for 5 minutes at 4°C. The supernatant was collected and transferred to a new centrifuge tube and centrifuged at 10,000 × g for 10 minutes at 4°C. The mitochondrial pellet was resuspended in 0.2 ml of mitochondrial extraction buffer, followed by centrifugation at 12,000 × g for 10 minutes at 4°C. The supernatant was discarded, and the mitochondrial pellet was resuspended in mitochondrial respiration buffer for subsequent use.

Mitochondrial Quality Control

The extracted mitochondria were quantified using a BCA Protein Assay Kit (23250, ThermoFisher). The integrity of the isolated mitochondria was assessed using the Mitochondrial Complex I(E-BC-K151-M , Elabscience) and III Activity Assay Kit (E-BC-K149-M , Elabscience), the mitochondrial membrane potential was measured using the Mitochondrial Membrane Potential Assay Kit with JC-1 (C2006, Byeotime), and the energy synthesis capacity was evaluated using an ATP Assay Kit (S0026, Byeotime).

Electron Microscopy

For transmission electron microscopy (TEM), the isolated mitochondria were fixed

overnight in 0.2 M sodium cacodylate buffer containing 2.5% formaldehyde, 5% glutaraldehyde, and 0.06% picric acid at pH 7.4. The samples were washed in cacodylate buffer, stained with 1% osmium tetroxide and 1.5% potassium ferricyanide, and then dehydrated using ethanol and propylene oxide. After infiltration and embedding in Epon-Araldite (Electron Microscopy Sciences, Hatfield, PA), sections (60-80 nm thick) were cut using an Ultracut-S ultramicrotome (Reichert Technologies, Depew, NY) and mounted on copper grids (200 mesh) for observation with a transmission electron microscope (Hitachi H-7500).

Mitochondrial Transplantation in Cells

After mitochondrial isolation, the mitochondria were quantified using a BCA Protein Assay Kit (23250, ThermoFisher). For co-culture, 10μg of mitochondria were added per 10^5 cells. For competitive mitochondrial internalization, 1 μg of mitochondria was added per 10^5 cells, with 0.5μg of each type for dual mitochondrial competition or 0.33μg of each type for triple mitochondrial competition.

Mitochondrial Internalization and Observation

Recipient cell membranes were labeled with WGA594 or WGA488, and the isolated exogenous mitochondria were labeled with MitoTracker™ Green FM or MitoTracker™ Red CMXRos. Both the cells and the exogenous mitochondria were washed twice with DPBS after 30 minutes. The mitochondria and cells were co-cultured for 24 hours in confocal dishes, fixed with paraformaldehyde containing DAPI, washed twice with DPBS, and observed using an inverted laser confocal microscope (LSM900 with Airyscan2, Zeiss).

ATP Content Measurement

ATP content was measured using an ATP Assay Kit (S0026, Beyotime) following the manufacturer's instructions. One hundred micrograms of isolated mitochondria or cells seeded in a 6-well plate (at a density of 5×10^5 cells/well) were treated with 200 μL of ATP lysis buffer, centrifuged at 12,000 × g for 5 minutes at 4°C. Twenty microliters of supernatant were mixed with 100 μL of ATP detection solution in a 96-well white solid flat-bottom polystyrene microplate (Corning) and the luminescence (RLU) was measured using a multifunctional microplate reader (Tecan).

Mitochondrial Membrane Potential Fluorescence Quantification

The isolated mitochondria were subjected to protein quantification, followed by mitochondrial membrane potential assessment using the Mitochondrial Membrane Potential Assay Kit with JC-1 (C2006, Byeotime). In brief, 50 μg of mitochondria were mixed with 90 μL of JC-1 staining solution (2 μM) and seeded into a 96-well plate. The mixture was thoroughly mixed, and the membrane potential was immediately measured using the BioTek Cytation5 Multifunctional Cell Imaging Microplate Reader (Agilent), with an excitation wavelength of 485 nm and an emission wavelength of 590 nm.

Measurement of Intracellular Reactive Oxygen Species

Cells were seeded at a density of 1×10^5 cells/well in a 24-well plate. After treating the cells with the respective conditions, exogenous mitochondria were co-cultured with the cells for 24 hours. The medium was then removed, and the cells were washed twice with DPBS. The cells were incubated with 10 μM DCFH-DA (Beyotime) or 5 μM MitoSOX Red at 37°C for 30 minutes. The stained cells were washed with PBS and observed using an inverted laser scanning confocal microscope (LSM900 with Airyscan2, Zeiss) or an inverted fluorescence microscope (EVOS M5000, ThermoFisher). The mitochondrial ROS fluorescence intensity was measured using a multifunctional microplate reader (Tecan) with an excitation wavelength of 510 nm and an emission wavelength of 580 nm.

Measurement of Mitochondrial Membrane Potential

Cells were seeded at a density of 1×10^5 cells/well in a 24-well plate. After treating the cells with the respective conditions, exogenous mitochondria were co-cultured with the cells for 24 hours. The medium was then removed, and the cells were washed twice with DPBS. Following the Mitochondrial Membrane Potential Assay Kit with JC-1 protocol, 500 μL of JC-1 staining solution (2 μM) was added to each well and incubated for 20 minutes. The cells were then washed and observed using an inverted laser scanning confocal microscope (LSM900 with Airyscan2, Zeiss) or an inverted fluorescence microscope (EVOS M5000, ThermoFisher) in phenol-red-free DMEM (Invitrogen).

CCK8 Assay

According to the Cell Counting Kit-8 (C0037, Beyotime) protocol, 100 μL of cell suspension (density of 1×10^4) was seeded in a 96-well plate. After treating the cells with the respective conditions, 10 μL of CCK8 reagent was added, and the cells were incubated at 37°C for 2 hours. The absorbance at 450 nm was measured using a multifunctional microplate reader (Tecan). The percentage of cell viability was calculated based on the average optical density (OD) of each group.

DNA Oxidative Damage Detection

The supernatant of the cultured cells was collected 24 hours after mitochondrial transplantation. The 8-OHdG concentration was measured using the 8-OHdG ELISA Kit (E-EL-0028, Elabscience), and absorbance at 450 nm was recorded to quantify DNA oxidative damage.

Immunoinflammatory Cytokines Detection

The supernatant of the cultured cells was collected 24 hours after mitochondrial transplantation. The concentrations of IL-6, IL-10, and TNF-α were measured using the Mouse IL-6 ELISA Kit (PI326, Byeotime), Mouse IL-10 ELISA Kit (PI522, Byeotime), and Mouse TNF-α ELISA Kit (PT512, Byeotime), respectively, according to the

manufacturer's instructions, with absorbance at 450 nm.

Measurement of NOS, MDA, GSH, SOD, ALT, AST, Cr

The supernatants of cultured cells post-mitochondrial transplantation or serum from model mice were collected. According to the manufacturer's instructions (NJJCBIO), the OD values for NOS(A014-2-2), MDA(A003-1-2), GSH(A005-1-2), SOD(A001-2-2), ALT(C010-2-1), AST(C009-2-1), and Cr(C011-2-1) were measured at 550nm, 532 nm, 412 nm, 550 nm, 505 nm, 510 nm, and 546 nm, respectively.

Cell Fusion

When cells reached high proliferation rates and good condition, 3×10^6 HL-1 and H9C2 cells were harvested separately. HL1 cells were stained with WGA647 and H9C2 cells with WGA594. The staining was performed at 37°C for 25 minutes, followed by two washes with DPBS. The cells were then mixed and centrifuged at 200 g for 5 minutes. The supernatant was removed, and pre-warmed 50% PEG1450 (P7181, Sigma) was gradually added while stirring the pellet. A total of 700 μL of 50% PEG1450 was added within 1 minute. The mixture was incubated at 37°C for 1 minute, and then 10 mL of DMEM was added to dilute the PEG1450. The centrifuge tube was placed in a 37°C incubator for 10 minutes before being centrifuged again at 200 g for 5 minutes. The cells were washed twice with DPBS, resuspended in complete culture medium, and incubated at 37°C with 5% CO_2 for 24-48 hours. Cell fusion was observed using an inverted laser scanning confocal microscope (LSM900 with Airyscan2, Zeiss), and fused HL1+H9C2 cells were sorted using a MoFlow XDP flow sorter (Beckman) for further culture.

Mitochondrial Competitive Internalization

For two types of mitochondrial competitive internalization, the mitochondria were stained with MitoTracker™ Deep Red FM and MitoTracker™ Green FM for 30 minutes, washed twice with DPBS, and co-cultured with recipient cells for 24 hours. The medium was replaced with phenol-red-free culture medium containing ProlongTM antifade reagent, and live-cell imaging was performed using an inverted laser scanning confocal microscope (LSM900 with Airyscan2, Zeiss). For three types of mitochondrial competitive internalization, mitochondria were stained with MitoTracker™ Deep Red FM, MitoTracker™ Green FM, and MitoTracker™ Red CMXRos for 30 minutes, washed twice with DPBS, and co-cultured with recipient cells for 24 hours. The medium was then replaced, and live-cell imaging was performed under the same conditions.

HIIT Functional Training

Six-month-old mice underwent one week of preconditioning exercise using a small animal treadmill (XR-PT-10B, Shxinruan) before beginning an 8-week HIIT training regimen. The maximum exercise capacity was tested weekly to adjust running speed. Each session began with a 10-minute warm-up at a speed of 10 m/min. For the first two weeks, the regimen

included high-intensity exercise at 24 m/min (80% VO2max) for 3 minutes, followed by 3 minutes of low-intensity recovery at 15 m/min with a 0° incline. In weeks 3-4, the regimen increased to 26 m/min (80% VO2max) for 3 minutes and 15 m/min for 3 minutes at an 8° incline. In weeks 5-6, the speed was further increased to 28 m/min (80% VO2max) for 3 minutes, followed by 17 m/min for 3 minutes at a 16° incline. Finally, in weeks 7-8, the speed reached 30 m/min (80% VO2max) for 3 minutes, followed by 17 m/min for 3 minutes at a 25° incline. Each session concluded with 8 minutes at 15 m/min. The regimen consisted of 7 sets (3+3) per session, with each session lasting 1 hour, 5 days per week, with 2 days of rest. Similarly, a 29-year-old healthy human (the author) underwent an 8-week HIIT training program, consisting of a 30-second maximal effort sprint (9+ on the 1–10 RPE scale) followed by a 4.5-minute low-intensity jog (4–5 on the 1–10 RPE scale), daily for 30 minutes, 5 days per week, with an additional 2 days of MICT running at 15 km/h for 30 minutes.

Aging Model

Two categories were used: disease-induced and normal aging. For the disease-induced model, 54 two-month-old C57BL/6J mice were divided into groups: D-gal, C2C12, Young C57, Trained People, Trained C57, and Wild Mice. Aging was induced by subcutaneous injection of D-gal at a dose of 500 mg/kg, once daily for 8 weeks. For the normal aging model, 27 four-month-old C57BL/6J mice were divided into Control, Young C57, and Wild Mice groups, with no drug treatment, and were kept under standard conditions.

Acute Inflammation Model

Two categories were used. For the inflammation model, 27 four-month-old C57BL/6J mice were divided into LPS, Young C57, and Wild Mice groups. Acute inflammation was induced by intraperitoneal injection of LPS at a dose of 2.5 mg/kg/day for 5 consecutive days. Another set of 27 four-month-old C57BL/6J mice was divided into Control, Young C57, and Wild Mice groups, with no drug treatment and normal rearing.

Animal Mitochondrial Transplantation

For the aging model, mitochondria were isolated from the gastrocnemius muscle tissues of Young C57, Trained People, Trained C57, and Wild Mice, as well as C2C12 cells, using the Mitochondria-Cytosol Protein Isolation Kit (C0010-50, Applygen). Mitochondrial protein was quantified using the BCA Protein Assay Kit (23250, ThermoFisher). A dose of 100μL/100μg of mitochondria was injected via the tail vein into the C2C12, Young C57, Trained People, Trained C57, and Wild Mice groups, while the control group received no treatment. For the normal type, mitochondria from Young C57 and Wild Mice were injected into their respective groups at the same dose, with the control group receiving 100μL of mitochondrial carrier solution. For the acute inflammation model, mitochondria were isolated from the gastrocnemius muscle of Young C57 and Wild Mice, quantified, and injected via the tail vein at a dose of 100μL/100μg into the Young C57 and Wild Mice

groups. The LPS group received no treatment, and the control group received 100μL of mitochondrial carrier solution.

Mitochondrial Biodistribution

Isolated mitochondria were labeled with MitoTracker™ Deep Red FM at room temperature for 20 minutes, washed twice with DPBS, and injected via the tail vein into mice. After 24 hours, the heart, liver, and kidneys were collected, and mitochondrial biodistribution was assessed using a multimodal small animal in vivo imaging system, PerkinElmer IVIS Spectrum (PerkinElmer).

Motor Function Detection（Rotarod Test）

Three days prior to the experiment, mice underwent adaptive training. During the formal experiment, mice were placed on a Rotating rod instrument (XR-6C/XR-6D, Shxinruan) at 5 rpm/min for 5 minutes, then gradually accelerated to 40 rpm/min. The time the mice remained on the rotating rod was recorded using a stopwatch until they fell off. The maximum duration for aging or acute inflammation mice was 180 seconds, with a maximum of 360 seconds for normal mice. Each mouse was tested three times with a 3-minute interval between trials, ensuring a quiet environment during the experiment.

Body Weight Measurement

All experimental groups of mice were weighed 3 days before and 1 week after mitochondrial transplantation, with weights recorded.

Mouse Forelimb Grip Strength Test

Three days prior to the experiment, mice underwent adaptive training. During the formal experiment, each mouse was placed on a Mouse grip tester (XR501, Shxinruan), and gentle traction was applied to the tail, prompting the mouse to grip the probe firmly with its forelimbs. The grip strength reading was recorded when the experimenter applied maximum force, with the experiment conducted in a quiet environment.

Lower Limb Muscle Volume and Injury Assessment

One week after mitochondrial injection, mice were briefly anesthetized with a mixture of isoflurane (3.0%) and O2 (2.0 L/min) via a nose cone and placed in a custom-made restraint tube, with the right lower limb fixed with a coil. During MRI imaging, mice were anesthetized with a mixture of isoflurane (1.5%) and O2 (0.6 L/min). The rectal temperature was maintained at 37 ± 1°C using a heated water blanket. A small animal magnetic resonance imaging system, PharmaScan70/16S (Bruker), was used to scan the horizontal plane of lower limb muscles, employing spin echo (SE) T1WI (TR4000ms, TE 28.5ms), fast spin echo (FSE) T2WI (TR4000ms, TE 47.5ms), with a slice thickness of 4 mm and an interval of 1 mm. Process the images using Paravision6.0.1 (Bruker).

Western Blot

Proteins were extracted from liver and kidney tissues, separated by 10% SDS-PAGE, and transferred onto polyvinylidene fluoride (PVDF) membranes. Phosphorylated proteins and total proteins were blocked with 5% BSA and 5% milk, respectively. PVDF membranes were incubated with primary antibodies at 4°C overnight, followed by a 2-hour incubation with HRP-conjugated secondary antibodies at room temperature. Gel imaging was performed using the Tanon-5200Multi automatic luminous system (Tanon).

Quantitative PCR

Twenty-four hours after mitochondrial transplantation, total RNA was extracted using Trizol reagent. Purified RNA was reverse-transcribed into cDNA using the PrimeScript™ RT reagent Kit (RR037Q, Takara). RT-qPCR was conducted with SYBR Green Master Mix (430915, Invitrogen) using the ABI QuantStudio 5 Real-Time PCR system (ThermoFisher). Expression levels were normalized to the internal control 18s rRNA. The primer sets are listed in Key resources table.

Quantification and Statistical Analysis

Cell experiments were repeated at least three times except for mitochondrial competitive internalization and animal experiments except for body weight measurement, grip strength and motor function tests. GraphPad Prism 9.01(GraphPad Software Inc., San Diego, CA, USA) software was used for statistical analysis. The data were expressed as mean ± standard error (SEM). For normally distributed data and comparisons between two groups, the significance was calculated using unpaired two-tailed Student's *t*-tests. Comparisons between three or more groups were performed using ordinary One-way ANOVA,Using Two-way ANOVA and Bonferroni post hoc test were used to compare multi-factor variance for multiple data. The significance threshold was determined by p value < 0.05, and the annotation was ns = no statistical significance, * = $p<0.05$, ** = $p<0.01$, *** = $p<0.001$, **** = $p<0.0001$.

ACKNOWLEDGMENTS

I sincerely thank the People's Hospital of Dongguan City, affiliated with Southern Medical University, for providing free access to experimental instruments. I also extend our gratitude to Dr. Guiming Chen from the Department of Pathology and Pathophysiology at Southern Medical University and Dr. Rong Wu from the School of Traditional Chinese Medicine for their technical support with mitochondrial tail vein injections. Additionally, I appreciate the assistance of Master Xin Heng in the experiments involving fluorescence microscopy for detecting reactive oxygen species and mitochondrial membrane potential. Moreover, I express strong condemnation towards those who deliberately sabotage others' experiments. I urge all laboratories to actively remove such unethical individuals. This

work was carried out with the author's full commitment, with all funding provided personally by the author. Consequently, there are several limitations in this study, for which we apologize. There are three main reasons why further experiments are challenging for me: first, the experimental cells were deliberately destroyed, preventing continuation; second, it is extremely difficult to obtain mitochondria from HIIT-trained and wild mice; third, and most importantly, there is a lack of funding. Due to my poor English proficiency, this paper was translated from Chinese to English by ChatGPT for submission. If there is anything unclear, please feel free to contact me. Alternatively, you can request the original Chinese manuscript and translate it yourselves. I can also add an additional corresponding author if needed. Let me know if you need any further adjustments! Should additional resources become available, I plan to conduct more detailed research to provide a more comprehensive explanation of my study. Therefore, if you like it, take it; if you don't, then fuck it.

Author Contribution

Xiaomeng Lu(fylxmgg@gmail.com) leads all the experimental design, experimental operation, experimental analysis, article writing and proofreading. Jiang Yong(18675838414@163.com) provided the experimental site and some experimental equipment.

DECLARATION OF INTERESTS

The authors declare no competing interests.

References

1. Ali Pour P, Kenney MC, Kheradvar A (2020) Bioenergetics Consequences of Mitochondrial Transplantation in Cardiomyocytes. *Journal of the American Heart Association* 9: e014501
2. Baharvand F, Habibi Roudkenar M, Pourmohammadi-Bejarpasi Z, Najafi-Ghalehlou N, Feizkhah A, Bashiri Aliabadi S, Salari A, Mohammadi Roushandeh A (2024) Safety and efficacy of platelet-derived mitochondrial transplantation in ischaemic heart disease. *International journal of cardiology* 410: 132227
3. Bamshad C, Habibi Roudkenar M, Abedinzade M, Yousefzadeh Chabok S, Pourmohammadi-Bejarpasi Z, Najafi-Ghalehlou N, Sato T, Tomita K, Jahanian-Najafabadi A, Feizkhah A, Mohammadi Roushandeh A (2023) Human umbilical cord-derived mesenchymal stem cells-harvested mitochondrial transplantation improved motor function in TBI models through rescuing neuronal cells from apoptosis and alleviating astrogliosis and microglia activation. *International immunopharmacology* 118: 110106
4. Bhattacharya D, Slavin MB, Hood DA (2023) Muscle mitochondrial transplantation can rescue and maintain cellular homeostasis. *American journal of physiology Cell*

physiology 325: C862-c884
5. Boutonnet L, Mallard J, Charles AL, Hucteau E, Gény B, Lejay A, Grandperrin A (2024) Autologous mitochondrial transplantation in male mice as a strategy to prevent deleterious effects of peripheral ischemia-reperfusion. *American journal of physiology Cell physiology* 326: C449-c456
6. Broughton RE, Reneau PC (2006) Spatial covariation of mutation and nonsynonymous substitution rates in vertebrate mitochondrial genomes. *Molecular biology and evolution* 23: 1516-24
7. Burki F (2016) Mitochondrial Evolution: Going, Going, Gone. *Current biology : CB* 26: R410-2
8. Butenko A, Lukeš J, Speijer D, Wideman JG (2024) Mitochondrial genomes revisited: why do different lineages retain different genes? *BMC biology* 22: 15
9. Chang JC, Chang HS, Wu YC, Cheng WL, Lin TT, Chang HJ, Kuo SJ, Chen ST, Liu CS (2019) Mitochondrial transplantation regulates antitumour activity, chemoresistance and mitochondrial dynamics in breast cancer. *Journal of experimental & clinical cancer research : CR* 38: 30
10. Chen T, Majerníková N, Marmolejo-Garza A, Trombetta-Lima M, Sabogal-Guáqueta AM, Zhang Y, Ten Kate R, Zuidema M, Mulder P, den Dunnen W, Gosens R, Verpoorte E, Culmsee C, Eisel ULM, Dolga AM (2023) Mitochondrial transplantation rescues neuronal cells from ferroptosis. *Free radical biology & medicine* 208: 62-72
11. Clark MA, Shay JW (1982) Mitochondrial transformation of mammalian cells. *Nature* 295: 605-7
12. Cohen NR, Lobritz MA, Collins JJ (2013) Microbial persistence and the road to drug resistance. *Cell host & microbe* 13: 632-42
13. Cruz-Gregorio A, Aranda-Rivera AK, Amador-Martinez I, Maycotte P (2023) Mitochondrial transplantation strategies in multifaceted induction of cancer cell death. *Life sciences* 332: 122098
14. Doulamis IP, Guariento A, Duignan T, Orfany A, Kido T, Zurakowski D, Del Nido PJ, McCully JD (2020) Mitochondrial transplantation for myocardial protection in diabetic hearts. *European journal of cardio-thoracic surgery : official journal of the European Association for Cardio-thoracic Surgery* 57: 836-845
15. Doulamis IP, Nomoto RS, Tzani A, Hong X, Duignan T, Celik A, Del Nido PJ, McCully JD (2022) Transcriptomic and proteomic pathways of diabetic and non-diabetic mitochondrial transplantation. *Scientific reports* 12: 22101
16. Dubinin MV, Mikheeva IB, Stepanova AE, Igoshkina AD, Cherepanova AA, Semenova AA, Sharapov VA, Kireev, II, Belosludtsev KN (2024) Mitochondrial Transplantation Therapy Ameliorates Muscular Dystrophy in mdx Mouse Model. *Biomolecules* 14
17. Eo H, Yu SH, Choi Y, Kim Y, Kang YC, Lee H, Kim JH, Han K, Lee HK, Chang MY, Oh MS, Kim CH (2024) Mitochondrial transplantation exhibits neuroprotective effects and improves behavioral deficits in an animal model of Parkinson's disease.

Neurotherapeutics : the journal of the American Society for Experimental NeuroTherapeutics 21: e00355

18. Fu Y, Liu H, Song C, Zhang F, Liu Y, Wu J, Wen X, Liang C, Ma K, Li L, Zhang X, Shao X, Sun Y, Du Y, Song Y (2015) Mangiferin regulates cognitive deficits and heme oxygenase-1 induced by lipopolysaccharide in mice. *International immunopharmacology* 29: 950-956
19. Fuchs CD, Radun R, Dixon ED, Mlitz V, Timelthaler G, Halilbasic E, Herac M, Jonker JW, Ronda O, Tardelli M, Haemmerle G, Zimmermann R, Scharnagl H, Stojakovic T, Verkade HJ, Trauner M (2022) Hepatocyte-specific deletion of adipose triglyceride lipase (adipose triglyceride lipase/patatin-like phospholipase domain containing 2) ameliorates dietary induced steatohepatitis in mice. *Hepatology (Baltimore, Md)* 75: 125-139
20. Ganote CE, Armstrong SC (2003) Effects of CCCP-induced mitochondrial uncoupling and cyclosporin A on cell volume, cell injury and preconditioning protection of isolated rabbit cardiomyocytes. *Journal of molecular and cellular cardiology* 35: 749-59
21. Gorick C, Debski A (2024) Mitochondrial transplantation for ischemic heart disease. *Nature nanotechnology*
22. Gray MW (2012) Mitochondrial evolution. *Cold Spring Harbor perspectives in biology* 4: a011403
23. Gray MW, Burger G, Lang BF (1999) Mitochondrial evolution. *Science (New York, NY)* 283: 1476-81
24. Guariento A, Piekarski BL, Doulamis IP, Blitzer D, Ferraro AM, Harrild DM, Zurakowski D, Del Nido PJ, McCully JD, Emani SM (2021) Autologous mitochondrial transplantation for cardiogenic shock in pediatric patients following ischemia-reperfusion injury. *The Journal of thoracic and cardiovascular surgery* 162: 992-1001
25. Hong S, Kim S, Kim K, Lee H (2023) Clinical Approaches for Mitochondrial Diseases. *Cells* 12
26. Hosseinian S, Ali Pour P, Kheradvar A (2022) Prospects of mitochondrial transplantation in clinical medicine: Aspirations and challenges. *Mitochondrion* 65: 33-44
27. Hsu CC, Wang CH, Wu LC, Hsia CY, Chi CW, Yin PH, Chang CJ, Sung MT, Wei YH, Lu SH, Lee HC (2013) Mitochondrial dysfunction represses HIF-1α protein synthesis through AMPK activation in human hepatoma HepG2 cells. *Biochimica et biophysica acta* 1830: 4743-51
28. Hu YM, Lu SZ, Li YS, Wang H, Shi Y, Zhang L, Tu ZC (2022) Protective effect of antioxidant peptides from grass carp scale gelatin on the H(2)O(2)-mediated oxidative injured HepG2 cells. *Food chemistry* 373: 131539
29. Javani G, Babri S, Farajdokht F, Ghaffari-Nasab A, Mohaddes G (2022) Mitochondrial transplantation improves anxiety- and depression-like behaviors in aged stress-

exposed rats. *Mechanisms of ageing and development* 202: 111632
30. Jiang X, Ji S, Yuan F, Li T, Cui S, Wang W, Ye X, Wang R, Chen Y, Zhu S (2023) Pyruvate dehydrogenase B regulates myogenic differentiation via the FoxP1-Arih2 axis. *Journal of cachexia, sarcopenia and muscle* 14: 606-621
31. Jiang XP, Elliott RL, Head JF (2015) Exogenous normal mammary epithelial mitochondria suppress glycolytic metabolism and glucose uptake of human breast cancer cells. *Breast cancer research and treatment* 153: 519-29
32. Jin M, Wang Y, Huang M, Lu Z, Wang Y (2014) Sulphation can enhance the antioxidant activity of polysaccharides produced by Enterobacter cloacae Z0206. *Carbohydrate polymers* 99: 624-9
33. Jin P, Jiang J, Zhou L, Huang Z, Nice EC, Huang C, Fu L (2022) Mitochondrial adaptation in cancer drug resistance: prevalence, mechanisms, and management. *Journal of hematology & oncology* 15: 97
34. Kaza AK, Wamala I, Friehs I, Kuebler JD, Rathod RH, Berra I, Ericsson M, Yao R, Thedsanamoorthy JK, Zurakowski D, Levitsky S, Del Nido PJ, Cowan DB, McCully JD (2017) Myocardial rescue with autologous mitochondrial transplantation in a porcine model of ischemia/reperfusion. *The Journal of thoracic and cardiovascular surgery* 153: 934-943
35. Kim S, Noh JH, Lee MJ, Park YJ, Kim BM, Kim YS, Hwang S, Park C, Kim K (2023) Effects of Mitochondrial Transplantation on Transcriptomics in a Polymicrobial Sepsis Model. *International journal of molecular sciences* 24
36. La Morgia C, Maresca A, Caporali L, Valentino ML, Carelli V (2020) Mitochondrial diseases in adults. *Journal of internal medicine* 287: 592-608
37. Lee JM, Hwang JW, Kim MJ, Jung SY, Kim KS, Ahn EH, Min K, Choi YS (2021) Mitochondrial Transplantation Modulates Inflammation and Apoptosis, Alleviating Tendinopathy Both In Vivo and In Vitro. *Antioxidants (Basel, Switzerland)* 10
38. Lelandais C, Albert B, Gutierres S, De Paepe R, Godelle B, Vedel F, Chétrit P (1998) Organization and expression of the mitochondrial genome in the Nicotiana sylvestris CMSII mutant. *Genetics* 150: 873-82
39. Levoux J, Prola A, Lafuste P, Gervais M, Chevallier N, Koumaiha Z, Kefi K, Braud L, Schmitt A, Yacia A, Schirmann A, Hersant B, Sid-Ahmed M, Ben Larbi S, Komrskova K, Rohlena J, Relaix F, Neuzil J, Rodriguez AM (2021) Platelets Facilitate the Wound-Healing Capability of Mesenchymal Stem Cells by Mitochondrial Transfer and Metabolic Reprogramming. *Cell metabolism* 33: 283-299.e9
40. Li Z, Cao X, Liu Z, Wu F, Lin C, Wang CM (2024) Therapeutic effect of mitochondrial transplantation on burn injury. *Free radical biology & medicine* 215: 2-13
41. Logan DC (2003) Mitochondrial dynamics. *The New phytologist* 160: 463-478
42. Mahler HR (1981) Mitochondrial evolution: organization and regulation of mitochondrial genes. *Annals of the New York Academy of Sciences* 361: 53-75
43. McCully JD, Cowan DB, Pacak CA, Toumpoulis IK, Dayalan H, Levitsky S (2009) Injection of isolated mitochondria during early reperfusion for cardioprotection.

American journal of physiology Heart and circulatory physiology 296: H94-h105
44. McCully JD, Del Nido PJ, Emani SM (2023) Mitochondrial transplantation: the advance to therapeutic application and molecular modulation. *Frontiers in cardiovascular medicine* 10: 1268814
45. Moskowitzova K, Shin B, Liu K, Ramirez-Barbieri G, Guariento A, Blitzer D, Thedsanamoorthy JK, Yao R, Snay ER, Inkster JAH, Orfany A, Zurakowski D, Cowan DB, Packard AB, Visner GA, Del Nido PJ, McCully JD (2019) Mitochondrial transplantation prolongs cold ischemia time in murine heart transplantation. *The Journal of heart and lung transplantation : the official publication of the International Society for Heart Transplantation* 38: 92-99
46. Nitsch L, Lareau CA, Ludwig LS (2024) Mitochondrial genetics through the lens of single-cell multi-omics. *Nature genetics* 56: 1355-1365
47. Picone P, Porcelli G, Bavisotto CC, Nuzzo D, Galizzi G, Biagio PLS, Bulone D, Di Carlo M (2021) Synaptosomes: new vesicles for neuronal mitochondrial transplantation. *Journal of nanobiotechnology* 19: 6
48. Raval PK, Martin WF, Gould SB (2023) Mitochondrial evolution: Gene shuffling, endosymbiosis, and signaling. *Science advances* 9: eadj4493
49. Reznick DN, Ricklefs RE (2009) Darwin's bridge between microevolution and macroevolution. *Nature* 457: 837-42
50. Schatz G (2012) The fires of life. *Annual review of biochemistry* 81: 34-59
51. Shang Q, Bian X, Zhu L, Liu J, Wu M, Lou S (2023) Lactate Mediates High-Intensity Interval Training-Induced Promotion of Hippocampal Mitochondrial Function through the GPR81-ERK1/2 Pathway. *Antioxidants (Basel, Switzerland)* 12
52. Song JH, Choi J, Hong YJ, La H, Hong TK, Hong K, Do JT (2022) Developmental Potency and Metabolic Traits of Extended Pluripotency Are Faithfully Transferred to Somatic Cells via Cell Fusion-Induced Reprogramming. *Cells* 11
53. Souza-Tavares H, Santana-Oliveira DA, Vasques-Monteiro IML, Silva-Veiga FM, Mandarim-de-Lacerda CA, Souza-Mello V (2024) Exercise enhances hepatic mitochondrial structure and function while preventing endoplasmic reticulum stress and metabolic dysfunction-associated steatotic liver disease in mice fed a high-fat diet. *Nutrition research (New York, NY)* 126: 180-192
54. Su Y, Zhu L, Yu X, Cai L, Lu Y, Zhang J, Li T, Li J, Xia J, Xu F, Hu Q (2016) Mitochondrial Transplantation Attenuates Airway Hyperresponsiveness by Inhibition of Cholinergic Hyperactivity. *Theranostics* 6: 1244-60
55. Sun C, Liu X, Wang B, Wang Z, Liu Y, Di C, Si J, Li H, Wu Q, Xu D, Li J, Li G, Wang Y, Wang F, Zhang H (2019) Endocytosis-mediated mitochondrial transplantation: Transferring normal human astrocytic mitochondria into glioma cells rescues aerobic respiration and enhances radiosensitivity. *Theranostics* 9: 3595-3607
56. Sun L, Zhao Z, Guo J, Qin Y, Yu Q, Shi X, Guo F, Zhang H, Sun X, Gao C, Yang Q (2024) Mitochondrial transplantation confers protection against the effects of ischemic stroke by repressing microglial pyroptosis and promoting neurogenesis. *Neural*

regeneration research 19: 1325-1335
57. Sun X, Gao R, Li W, Zhao Y, Yang H, Chen H, Jiang H, Dong Z, Hu J, Liu J, Zou Y, Sun A, Ge J (2021) Alda-1 treatment promotes the therapeutic effect of mitochondrial transplantation for myocardial ischemia-reperfusion injury. *Bioactive materials* 6: 2058-2069
58. Tripathi K, Ben-Shachar D (2024) Mitochondria in the Central Nervous System in Health and Disease: The Puzzle of the Therapeutic Potential of Mitochondrial Transplantation. *Cells* 13
59. Ulger O, Kubat GB, Cicek Z, Celik E, Atalay O, Suvay S, Ozler M (2021) The effects of mitochondrial transplantation in acetaminophen-induced liver toxicity in rats. *Life sciences* 279: 119669
60. Volchuk A, Ye A, Chi L, Steinberg BE, Goldenberg NM (2020) Indirect regulation of HMGB1 release by gasdermin D. *Nature communications* 11: 4561
61. Yao X, Ma Y, Zhou W, Liao Y, Jiang Z, Lin J, He Q, Wu H, Wei W, Wang X, Björklund M, Ouyang H (2022) In-cytoplasm mitochondrial transplantation for mesenchymal stem cells engineering and tissue regeneration. *Bioengineering & translational medicine* 7: e10250
62. Yu Z, Hou Y, Zhou W, Zhao Z, Liu Z, Fu A (2021) The effect of mitochondrial transplantation therapy from different gender on inhibiting cell proliferation of malignant melanoma. *International journal of biological sciences* 17: 2021-2033
63. Zhang A, Liu Y, Pan J, Pontanari F, Chia-Hao Chang A, Wang H, Gao S, Wang C, Chang AC (2023) Delivery of mitochondria confers cardioprotection through mitochondria replenishment and metabolic compliance. *Molecular therapy : the journal of the American Society of Gene Therapy* 31: 1468-1479
64. Zhu Z, Li X, Wang X, Zuo X, Ma Y, Gao X, Liang Z, Zhang Z, Song Z, Ding T, Ju C, Li P, Li K, Zhang J, Quan H, Wang Z, Hu X (2023) Photobiomodulation augments the effects of mitochondrial transplantation in the treatment of spinal cord injury in rats by facilitating mitochondrial transfer to neurons via Connexin 36. *Bioengineering & translational medicine* 8: e10473

Key resources table

REAGENT or RESOURCE	SOURCE	IDENTIFIER
Antibodies		
anti-p65	Abcam	Cat# ab32536；RRID:AB_776751
anti-phospho-p65	Cell Signaling	Cat# 3033S；RRID:AB_2341216
anti-JNK	Cell Signaling	Cat# 9252S；RRID:AB_2250373
anti-phospho-JNK	Cell Signaling	Cat# 9251S；RRID:AB_823588
Goat Anti-Rabbit IgG (HL)	Abmart	Cat# M213811S；RRID:AB_2920649
Chemicals, peptides, and recombinant proteins		
Wheat Germ Agglutinin (WGA594)	ThermoFisher	Cat# W11262
Wheat Germ Agglutinin (WGA488)	ThermoFisher	Cat# W11261
Wheat Germ Agglutinin (WGA647)	ThermoFisher	Cat# W32466
MitoTracker™ Deep Red FM	ThermoFisher	Cat# M22426
MitoTracker™ Green FM	ThermoFisher	Cat# M7514
MitoTracker™ Red CMXRos	ThermoFisher	Cat# M7512
Prolong™ Anti-fluorescence quencher	Invitrogen	Cat# P36975
LPS	Sigma Aldrich	Cat# L2880
H2O2	Sigma Aldrich	Cat# 323381
CCCP	Abcam	Cat# ab141229
D-gal	MCE	Cat# HY-N0210
MitoSox Red	MCE	Cat# HY-D1055
$HgCL_2$	Sinoreagent	Cat# 10013616
Critical commercial assays		
Mitochondria-Cytosol Protein Isolation Kit	Applygen	Cat# C0010-50
Plant mitochondrial Extraction Kit	Solarbio	Cat# SM0020
ATP Assay Kit	Beyotime	Cat# S0026
Mitochondrial membrane potential assay kit with JC-1	Beyotime	Cat# C2006
Cell Counting Kit-8	Beyotime	Cat# C0037
Mouse IL-6 ELISA Kit	Beyotime	Cat# PI326
Mouse IL-10 ELISA Kit	Beyotime	Cat# PI522

Mouse TNF-α ELISA Kit	Beyotime	Cat# PT512
Mitochondrial complex III Activity Assay Kit	Elabscience	Cat# E-BC-K149-M
Mitochondrial complex I Activity Assay Kit	Elabscience	Cat# E-BC-K151-M
Superoxide Dismutase (SOD) typed assay kit	NJJCBIO	Cat# A001-2-2
Malondialdehyde (MDA) assay kit	NJJCBIO	Cat# A003-1-2
Glutathione Peroxidase (GSH-PX) assay kit	NJJCBIO	Cat# A005-1-2
Total Nitric Oxide Synthase assay kit	NJJCBIO	Cat# A014-2-2
Aspartate aminotransferase Assay Kit	NJJCBIO	Cat# C010-2-1
Alanine aminotransferase Assay Kit	NJJCBIO	Cat# C009-2-1
Creatinine (Cr) Assay kit	NJJCBIO	Cat# C011-2-1
Peg1450（50%）	Sigam Aldrich	Cat# P7181
BCA Protein Assay Kit	ThermoFisher	Cat# 23250
SYBR™ Green PCR Master Mix	ThermoFisher	Cat# 4309155
PrimeScript™ RT reagent Kit	Takara	Cat# RR037Q
Experimental models: Cell lines		
MDBK	ATCC	Cat# GNO7
MDCK	ATCC	Cat# GNO23
Vero	ATCC	Cat# SCSP-520
PK15	ATCC	Cat# GNO31
LMH	Sunncell	Cat# SNL-494
Sf9	Procell	Cat# CL-0205
L929	Procell	Cat# CL-0089
H9C2	ATCC	Cat# GNR5
HL1	ATCC	Cat# GNM46
AC16	ATCC	Cat# SCSP-555
HepG2	ATCC	Cat# SCSP-510
C2C12	ATCC	Cat# SCSP-505
BMDM	This paper	N/A
CRFK	ATCC	Cat# GNO16
Experimental models: Organisms/strains		
Mouse: C57BL/6J	Southern Medical University	N/A
Oligonucleotides		
Mouse 18S rRNA RT-qPCR Forward： CGATCCGAGGGCCTCACTA Reverse：	This paper	N/A

AGTCCCTGCCCTTTGTACACA		
Mouse IL-4 RT-qPCR Forward： ATGGGTCTCACCTCCCAACTG Reverse： TCAGCTCGAACACTTTGAATATTTC TCTCTCAT	This paper	N/A
Mouse IL-6 RT-qPCR Forward： CCAGAGTCCTTCAGAGAGATACA Reverse： CCTTCTGTGACTCCAGCTTATC	This paper	N/A
Mouse IL-8 RT-qPCR Forward： ATGACTTCCAAGCTGGCCGTG Reverse： TTATGAATTCTCAGCCCTCTTCAAA AACTTCTC	This paper	N/A
Mouse IL-13 RT-qPCR Forward： TGAGCAACATCACACAAGACC Reverse： GGCCTTGCGGTTACAGAGG	This paper	N/A
Mouse IL-18 RT-qPCR Forward： GAAGGACACTTTCTTGCTTGC Reverse： GTGAGAGTGAACATTACAGATTTAT CC	This paper	N/A
Mouse IL-1β RT-qPCR Forward： GGTGTGTGACGTTCCCATTA Reverse： ATTGAGGTGGAGAGCTTTCAG	This paper	N/A
Mouse TGF-β RT-qPCR Forward： ATGACACCACCTGAACGTCTCTTC Reverse： CTACAGAGCGAAGGCTCCAAAGAA GACAGTACT	This paper	N/A
Mouse SOD1 RT-qPCR Forward： AACCAGTTGTGTTGTCAGGAC Reverse： CCACCATGTTTCTTAGAGTGAGG	This paper	N/A
Mouse HMGB1 RT-qPCR Forward： GCTGACAAGGCTCGTTATGAA Reverse： CCTTTGATTTTGGGGCGGTA	This paper	N/A
Mouse COX1 RT-qPCR	This	N/A

Forward： GACCGCAATGAACTTCGGGA Reverse： TCCATTAGGTCTCTAAAGCCGAG	paper	
Mouse ARG1 RT-qPCR Forward： CTCCAAGCCAAAGTCCTTAGAG Reverse： GGAGCTGTCATTAGGGACATCA	This paper	N/A
Mouse MPO RT-qPCR Forward： CGACATTCTGCCTGGATAAGG Reverse： TCTCGAACACTCTCCATTTGC	This paper	N/A
Mouse CCL5 RT-qPCR Forward：TTTGCCTACCTCTCCCTCG Reverse： CGACTGCAAGATTGGAGCACT	This paper	N/A
Mouse CCL1 RT-qPCR Forward： TGCCGTGTGGATACAGGATG Reverse： GTTGAGGCGCAGCTTTCTCTA	This paper	N/A
Mouse CXCL1 RT-qPCR Forward： CCGAAGTCATAGCCACACTCA Reverse： CTCCGTTACTTGGGGACACC	This paper	N/A
Mouse CXCL2 RT-qPCR Forward： CCAACCACCAGGCTACAGG Reverse： GCGTCACACTCAAGCTCTG	This paper	N/A
Software and algorithms		
GraphPad Prism 9.0.1	GraphPad Software	https://www.graphpad.com/
Flowjo10.8.1	BD Biosciences	https://www.flowjo.com/
ImageJ	NIH Image for the Macintosh	https://imagej.nih.gov/ij/index.html
Image Lab6.0.1	Bio-Rad	https://www.bio-rad.com/
ZEISS Zen3.3	ZEISS	https://www.zeiss.com.cn/microscopy/l/campaigns/software/2023/zeiss-zen.html
7500Software v2.3	ThermoFisher	https://www.thermofisher.cn/cn/zh/home/technical-resources/software-downloads/applied-biosystems-7500-real-time-pcr-system.html

Paravision6.0.1	Bruker	https://www.bruker.com/zh/products-and-solutions/preclinical-imaging/paravision-360.html
Other		
PerkinElmer IVIS Spectrum	PerkinElmer	Custom
EVOS M5000	ThermoFisher	Custom
PharmaScan70/16S	Bruker	Custom
Thermo Scientific EVOS M5000	ThermoFisher	Custom
MoFlow XDP flow sorter	Beckman	Custom
Hitachi H-7500	Hitachi	Custom
LSM900 with Airyscan2	Zeiss	Custom
ABI QuantStudio 5	ThermoFisher	Custom
Multifunctional microplate reader	Tecan	Custom
BioTek Cytation5	Agilent	Custom
Tanon-5200Multi	Tanon	Custom
Rotating rod instrument	Shxinruan	Cat# XR-6C/XR-6D
Mouse grip tester	Shxinruan	Cat# XR501
Small animal treadmill	Shxinruan	Cat# XR-PT-10B